https://doi.org/10.5194/nhess-2022-66
Preprint. Discussion started: 22 March 2022

Natural Hazards and Earth System Sciences Discussions

Site Characterization vis-à-vis Probabilistic Seismic Hazard and Disaster Potential Modelling in the Himalayan and Sub-Himalayan Tectonic Ensemble from Kashmir Himalaya to Northeast India at the backdrop of the updated Seismic Hazard of the Indian Subcontinent

Sankar Kumar Nath*, Anand Srivastava, Arpita Biswas, Jyothula Madan, Chitralekha Ghatak, Arnab Sengupta, Pritam Singh and Siddhartha Bhaumick
Department of Geology & Geophysics, Indian Institute of Technology Kharagpur, West Medinipur, 721302, India
*Correspondence to: Sankar Kumar Nath (nath@gg.iitkgp.ac.in)

Abstract. The Indian landmass comprising of three broad morphotectonic provinces, namely the Himalaya and Tertiary mobile belts, Indo-Gangetic Foredeep and Peninsular shield have been jolted time and again by catastrophic earthquakes. The Socio-economic Risk Map of India generated by integrating vulnerable exposures with the IBC-compliant surface-consistent Probabilistic Seismic Hazard through an Analytic Hierarchy Process and expert judgement places the entire Himalayan stretch comprising of Kashmir Himalaya, Northwest India, Nepal together with Indo-Gangetic Foredeep, Bengal Basin, Darjeeling-Sikkim Himalaya, Northeast India and Bhutan in 'High' to 'Severe' Risk regime thus presenting this Tectonic Ensemble a typical case for site-specific study. Combined surface and downhole Geophysical and Geotechnical measurements classify this Tectonic Ensemble into site classes F/E, D4, D3, D2, D1, C4, C3, C2, C1, B and A with spectral site amplifications of 6.2, 4.8, 4.2, 3.9, 3.3, 2.58, 2.2, 1.87, 1.81, 1.4 and 1.2 respectively at 0.73 - 8.5 Hz frequency range thus facilitating surface-consistent probabilistic seismic hazard assessment in this Tectonic Ensemble exhibiting a PGA variation of 0.06 to 1.99g whose structural impact is exhibited through SELENA-based building damage modelling using capacity spectrum method on the prevalent building types as 'none', 'slight', 'moderate', 'extensive' and 'complete' for all cities in the Ensemble.

Keywords: Socio-economic Seismic Risk, Surface-Consistent Probabilistic Seismic Hazard, Site Classification, Spectral Site Amplification, Damage Potential Modelling, SELENA.

1 Introduction

Earthquakes are a huge threat to humankind, claiming lives of thousands of people every year in various regions of the world. The Indian Peninsula is unquestionably one of the world's most earthquake-prone terrains. The Himalayas were uplifted when the Indian plate has been migrated northward and collided with the Eurasian plate. The collision caused huge tension in the crust, which is relieved occasionally by earthquakes along the plate boundary as well as intraplate faults and lineaments. Numerous earthquake-related disasters in India have demonstrated the seismic susceptibility of the country. It is mentioned in the Vulnerability Atlas of India published by Building Materials and Technology Promotion Council (BMTPC,

https://doi.org/10.5194/nhess-2022-66
Preprint. Discussion started: 22 March 2022


Natural Hazards and Earth System Sciences Discussions

2019), that more than 59% of the country's total land-cover is vulnerable to seismic threat. Unplanned urbanizations are fast emerging across the country to accommodate the burgeoning population. If the overall count of lost lives in the 2004 Sumatra earthquake of M_w 9.1 is considered, the death toll will reach to almost 43 thousand. Moderate sized earthquakes of M_w<7.0 have also wreaked havoc in the country, owing to structures that were not built as per prescribed building code to withstand the impact of likely earthquakes. The 2001 Bhuj earthquake of M_w 7.6 caused a total economic loss of roughly US$4600 million. **Figure 1** illustrates a juxtaposition of population data, locations of significant earthquakes and urban exposure. The fatality counts in urban settlements due to future great Himalayan earthquakes have been envisaged to be around 150-200 thousand. The consequences of large earthquakes are determined by their proximity to and vulnerable exposures of the built environment.

Figure 1 Significant earthquakes in India and its surrounding region illustrated with approximate epicentre locations together with corresponding casualty on the backdrop of population density distribution and urban exposure from the Centre for International Earth Science Information Network (CIESIN, 2010; Nath, 2017) for the year 2005.

The Indian subcontinent has a composite tectonic and geological setting as presented in **Fig. 2** depicting the major fault system and major lineament framework which has been identified as neotectonic features extracted by image processing techniques using multi-spectral Landsat TM, MSS, ETM, LISS-III & IV images, SRTM and Cartosat DEM data based on which and the underlying past seismic activities the India has been categorized into eleven major Seismogenic Tectonic Provinces viz. Z-I: Bengal Basin, Z-II: Indo-Gangetic Foredeep, Z-III: Central India, Z-IV: Kutch region, Z-V: Koyna-Warna region, Z-VI: Western Ghats, Z-VII: Eastern Ghats, Z-VIII: Kashmir Himalaya, Z-IX: Northwest India, Z-X: Darjeeling-Sikkim Himalaya and Z-XI: Northeast India which have the potential of generating moderate to large magnitude earthquakes as depicted in **Fig. 2**.

For any successful seismotectonic and seismic hazard investigation project, records of earthquake occurrences, termed as an earthquake catalogue serve as an important database. Nath et al. (2017) developed a homogeneous M_w based declustered earthquake catalogue of Southeast Asia and the surrounding region considering earthquake recordings spanning over the period of 1900-2014. The uniform magnitude scaling in moment magnitude M_w in this catalogue is accomplished through correlating various magnitude types. These correlations are established by Orthogonal Standard Regression (OSR) analysis on available data-pairs and have been compared with the existing relationships published previously. Subsequently, this catalogue has been declustered to obtain the foreshocks, mainshocks and aftershocks, with only the mainshocks kept as shown in **Fig. 3** that depicts 64,153 mainshock events in the region, which has further been extended to 2018 for Seismic Hazard, Vulnerability and Risk Assessment of the region performed here.

Figure 2 Eleven Major Seismogenic Tectonic Provinces marked as ‘Z-I to Z-XI’ on the Regional Seismotectonic Map of India (Nath, 2017).

https://doi.org/10.5194/nhess-2022-66
Preprint. Discussion started: 22 March 2022

Natural Hazards and Earth System Sciences Discussions

Figure 3 Declustered seismicity map of India and its surrounding region considered from an earthquake catalogue spanning over 1900-2018 depicting 64,153 Mainshock Events (after Nath et al., 2017).

2 Updated Probabilistic Seismic Hazard and IBC compliant Surface-consistent Risk of India and its surrounding region vis-à-vis the Seismogenic Tectonic Ensemble from Kashmir Himalaya to Northeast India

Several countries have implemented Probabilistic Seismic Hazard (PSH) mapping considering various seismic hazard components viz. the seismogenic source models both areal and/or tectonic, maximum earthquake prognosis through seismicity analysis using Bayesian equation of Frequency magnitude distribution (Kijko, 2004; Kijko and Graham, 1998), seismic site characteristics (Maiti et al. 2017), spectral and absolute ground motion prediction equations (Maiti et al. 2017; Nath et al. 2014; Nath and Thingbaijam 2012) etc. Most of the previous studies including Nath and Thingbaijam (2012) never considered fault and lineament based sources in their approach. In this updated probabilistic method whose protocol is shown in **Fig. 4**, the analysis explicitly incorporates all kinds of seismogenic sources and their activity rates, various threshold magnitudes obtained through seismicity analysis of the complete earthquake catalogue, a host of local, regional and global ground motion prediction equations and next generation attenuation models with well-defined aleatory and epistemic uncertainties associated with all the hazard components and their probability distributions. Employing the formulations of Cornell (1968), Esteva (1970) and McGuire (1976) a Logic Tree Framework of the type given in **Fig. 5** is worked out for the entire Indian peninsula and also used for the Tectonic Ensemble comprising of Kashmir Himalaya, Northwest India, Nepal Himalaya, Indo-Gangetic Foredeep, Bengal Basin, Darjeeling Sikkim Himalaya, Northeast India and Bhutan Himalaya which uses active tectonic features (i.e. faults and lineaments) in the 0-25 km, 25-70km, 70-180km and 180-300 km depth ranges and 172 layered polygonal sources demarcated in the same depth ranges with 60% and 40% weightage, M_w 3.5, 4.5 and 5.5 threshold magnitudes (Nath and Thingbaijam, 2012; Nath et al., 2014; Maiti et al., 2017; Nath et al., 2019; Nath et al. 2021a), smoothening seismicity-based activity rate computations using the formulations of Frankel (1995) for all the sources used here as shown in **Fig. S1** for the polygonal seismogenic sources at all the four depth levels and **Fig. S2** for a group of active tectonic features inscribed in each polygonal areal seismogenic sources in the 0-25 km focal depth range for the threshold magnitude of M_w 3.5 (Nath, 2017) in the electronic supplementary material and a host of Ground Motion Prediction Equations (GMPEs) and indigenously prepared spectral Next Generation Attenuation Models (NGAs) in 11 Seismogenic Tectonic Provinces (Nath et al., 2009; Nath et al., 2012; Nath et al., 2014; Adhikari and Nath, 2016; Nath, 2017; Maiti et al., 2017; Nath et al., 2019) as given in **Table S1** in the electronic supplementary material. The seismicity model parameters have been assigned weights of 0.36 with the respective ±1 standard deviation assigned weight equal to 0.32. Similar weight allotments (Grünthal and Wahlström, 2006) have been done for M_{max} as well. All the GMPEs and NGAs have gone through efficacy test using log-likelihood, LLH (Scherbaum et al., 2009) computations for ranking and weight assignments. The probability density functions for the magnitudes, epicentre distances and GMPEs follow standard probability density functions as used by Nath and Thingbaijam (2012).

https://doi.org/10.5194/nhess-2022-66
Preprint. Discussion started: 22 March 2022

Natural Hazards and Earth System Sciences Discussions

Figure 4 Computational Protocol for Probabilistic Seismic Hazard Assessment of an Earthquake County comprising of several Seismogenic Tectonic Provinces.

Figure 5 A typical logic tree formulation for computing Probabilistic Seismic Hazard at each node of the Study Region (modified from Nath and Thingbaijam, 2012).

The updated Probabilistic Seismic Hazard (PSH) of India at firm rock site condition is seen to vary from 0.05g to 0.95g for 10% probability of exceedance in 50 years as depicted in **Fig. 6(a)** and 0.074 to 1.56g for 2% probability of exceedance in 50 years as shown in **Fig. 6(b)**. The cities of Bangalore, Chennai, Hyderabad, Vijayawada, Vishakhapatnam and Puducherry located in the Eastern Ghat Seismogenic Tectonic Province Z-VII, Kochi & Thiruvananthapuram located in the Western Ghat Seismogenic Tectonic Province Z-VI, Mumbai & Pune located in the Koyna-Warna Seismogenic Tectonic Province Z-V, Jaipur & Amritsar lying in the Northwest Seismogenic Tectonic Province Z-IX, Allahabad, Patna, Lucknow, New Delhi lying in the Indo-Gangetic Seismogenic Tectonic Province Z-II, Bhopal, Nagpur and Raipur located in the Central India Seismogenic Tectonic Province Z-III, Jamshedpur & Bhubaneswar lying in the Bengal Basin Seismogenic Tectonic Province Z-I, all exhibit low hazard level with PGA varying from 0.050.25g for 10% probability of exceedance in 50 years. The cities of Koyna on the other hand, located in the Koyna-Warna Seismogenic Tectonic Province Z-V, Kolkata, Dhaka and Chittagong located in the Bengal Basin Seismogenic Tectonic Province Z-I exhibit moderate hazard level of the order of PGA 0.25 to 0.45g for 10% probability of exceedance in 50 years. The cities of Ahmedabad, Bhavnagar, Surat, Vadodara lying in the Kutch Seismogenic Tectonic Province Z-IV, Jammu lying in the Kashmir Himalaya Seismogenic Tectonic Province Z-VIII, Thimphu lying in the Bhutan Himalaya, Gangtok lying in the Darjeeling-Sikkim Himalaya Seismogenic Tectonic Province Z-X present high PGA level of the order of 0.45 to 0.65 for 10% probability of exceedance in 50 years. The cities of Srinagar located in the Kashmir Himalaya Seismogenic Tectonic Province Z-VIII, Kathmandu in the Nepal Himalaya, Aizawl & Imphal located in the Northeast India Seismogenic Tectonic Province Z-XI all exhibit very high PSH level with PGA varying between 0.65-0.80g for 10% probability of exceedance in 50 years. The cities of Bhuj located in the most seismogenic Kutch Tectonic Province Z-IV, Guwahati, Dispur and Shillong located in the most seismogenic Northeast India Tectonic Province Z-XI exhibit severe hazard level to the tune of PGA ranging from 0.80 to 0.95g for 10% probability of exceedance in 50 years. Similar hazard level is observed to be prevalent in all the Seismogenic Tectonic Provinces for the maximum hazard scenario for 2% probability of exceedance in 50 years as evident from **Fig. 6(b)**.

Figure 6 Probabilistic Seismic Hazard of India and its surrounding region in terms of Peak Ground Acceleration (PGA) at Bedrock level for (**a**) 10% Probability of exceedance in 50 years and (**b**) 2% Probability of exceedance in 50 years.

Spatial distribution of Pseudo Spectral Acceleration (PSA) for 0.2sec, 0.3sec and 1.0sec at engineering bedrock for both 10% and 2% probability of exceedance in 50 years for the entire Indian Peninsula have been computed and presented in **Figs. 7**, **8** and **9** respectively as necessitated for working out 5% damped design response spectra following International Building Code (IBC, 2009) and structural impact assessment using SELENA (Molina et al., 2014).

https://doi.org/10.5194/nhess-2022-66
Preprint. Discussion started: 22 March 2022


Natural Hazards and Earth System Sciences Discussions

Figure 7 Probabilistic Seismic Hazard of India and its surrounding region in terms of Pseudo Spectral Acceleration (PSA) at Bedrock level for 0.2 sec period for (**a**) 10% Probability of exceedance in 50 years and (**b**) 2% Probability of exceedance in 50 years.

Figure 8 Probabilistic Seismic Hazard of India and its surrounding region in terms of Pseudo Spectral Acceleration (PSA) at Bedrock level for 0.3 sec period for (**a**) 10% Probability of exceedance in 50 years and (**b**) 2% Probability of exceedance in 50 years.

Figure 9 Probabilistic Seismic Hazard of India and its surrounding region in terms of Pseudo Spectral Acceleration (PSA) at Bedrock level for 1.0 sec period for (**a**) 10% Probability of exceedance in 50 years and (**b**) 2% Probability of exceedance in 50 years.

In order to manifest the implications of this probabilistic seismic hazard, preliminary socio-economic seismic risk of India is calculated based on the vulnerability exposures on Building Density & Population Density according to Census of India (Chandramouli and General, 2011), Landuse/Landcover abbreviated as LULC (Karra et al., 2021) of IBC-compliant (IBC, 2009) site class-based bedrock amplified surface PGA(g) distribution with 10% probability of exceedance in 50 years, therein all integrated through Analytic Hierarchy Process, AHP (Reveshti and Gharakhlou, 2009; Ishita and Khandakar, 2010; Panahi et al., 2012; Karimzadeh et al., 2014; Nath et al., 2015; Nath et al., 2021b) with weight and rank assignments to each individual theme performed through pairwise comparison and expert judgement as shown in **Fig. 10.**

Figure 10 Seismic Risk Assessment of India on GIS platform through integration of (**a**) Population Density, (**b**) Building Density, (**c**) IBC compliant Surface PGA (in g) distribution with 10% probability of exceedance in 50 years and (**d**) Landuse/Landcover (LULC) thereby generating Socio-economic Seismic Risk Map of India as shown in (**e**). The weight assignment in the integration protocol is performed through pairwise comparison and expert judgement.

The Socio-Economic Risk (SER) thus computed for India has been categorized into five zones, viz. 'Low with SER≤0.2', 'Moderate with 0.2<SER≤0.4', 'High with 0.4<SER≤0.6', 'Very High for 0.6<SER≤0.8' and 'Severe 0.8<SER≤1.0)'. The cities of Srinagar and Jammu lying in the Kashmir Himalaya Seismogenic Tectonic Province Z-VIII, Chandigarh, Dehradun, Shimla, Gurugram and Ludhiana located in the Northwest India Tectonic Province Z-IX, Patna, Lucknow, New Delhi, Agra and Gaya lying in the Indo-Gangetic Foredeep Seismogenic Tectonic Province Z-II, Kolkata located in the Bengal Basin Seismogenic Tectonic Province Z-I, Kachchh, Bhuj and Rajkot located in the Kutch Seismogenic Tectonic Province Z-IV, Mumbai, Pune, Koyna and Latur located in the Koyna-Warna Seismogenic Tectonic Province Z-V, Bangalore lying in the Eastern Ghat Seismogenic Tectonic Province Z-VII, Kochi located in the Western Ghat Seismogenic Tectonic Province Z-VI, Gangtok and Darjeeling located in the Darjeeling-Sikkim Himalaya Seismogenic Tectonic Province Z-X, Guwahati, Dispur, Shillong, Aizawl, Agartala, Kohima, Imphal and Itanagar located in the Northeast India Seismogenic Tectonic Province Z-XI, all exhibit 'Severe Risk' level. The cities of Leh and Ladakh lying in the Kashmir Himalaya Seismogenic Tectonic Province Z-VIII, Amritsar, Udaipur and Jaipur located in the Northwest India Seismogenic Tectonic Province Z-

https://doi.org/10.5194/nhess-2022-66
Preprint. Discussion started: 22 March 2022


Natural Hazards and Earth System Sciences Discussions

IX, Allahabad and Varanasi lying in the Indo-Gangetic Foredeep Seismogenic Tectonic Province Z-II, Surat, Ahmedabad and Gandhinagar located in the Kutch Seismogenic Tectonic Province Z-IV, Hyderabad and Chennai lying in the Eastern Ghat Seismogenic Tectonic Province Z-VII, Kozhikode located in the Seismogenic Western Ghat Tectonic Province Z-VI, all show 'Very High Risk' level. The cities of Bikaner and Jaisalmer located in the Northwest India Seismogenic Tectonic Province Z-IX, Jamshedpur located in the Bengal Basin Seismogenic Tectonic Province Z-I, Bhopal, Nagpur and Indore located in the Central India Seismogenic Tectonic Province Z-III, Nashik located in the Koyna-Warna Seismogenic Tectonic Province Z-V, Puducherry and Vijaywada lying in the Eastern Ghat Seismogenic Tectonic Province Z-VII, Thiruvananthapuram located in the Western Ghat Seismogenic Tectonic Province Z-VI, all exhibit 'High Risk' level where as The cities of Jodhpur located in the Northwest India Seismogenic Tectonic Province Z-IX, Cuttack and Bhubneswar located in the Bengal Basin Seismogenic Tectonic Province Z-I, Raipur located in the Central India Seismogenic Tectonic Province Z-III, Tiruchirappalli and Vishakhapatnam lying in the Eastern Ghat Seismogenic Tectonic Province Z-VII, all exhibit 'Low to Moderate Risk' level. This Socio-economic Risk Map of India places the Seismogenic Tectonic Ensemble comprising of Tectonic Provinces of Kashmir Himalaya Z-VIII, Northwest India Z-IX, Nepal Himalaya, Indo-Gangetic Foredeep region Z-II, Bengal Basin Z-I including Bangladesh, Darjeeling-Sikkim Himalaya Z-X, Northeast India Z-XI and Bhutan Himalaya in the "High" to "Severe" Risk regime thus presenting it a model case for site-specific surface-consistent Probabilistic Seismic Hazard study towards elevating bedrock probabilistic PGA distribution shown in **Fig. 11** to its surface-consistent level for a 475 years' of return period. The computed Seismic Hazard curves in this diagram depict the probability of exceeding both 10% and 2% in 50 years with a return period of 475 and 2475 years for various ground motion parameters at some representative selected cities viz. Srinagar, Amritsar, Kanpur, Chittagong, Itanagar and Thimphu as presented in **Fig. 11**.

Figure 11 Bedrock level Probabilistic Seismic Hazard of the Seismogenic Tectonic Ensemble comprising of Kashmir Himalaya to Northeast India, which encompasses Northwest India, Nepal Himalaya, Indo-Gangetic Foredeep, Darjeeling-Sikkim Himalaya, Bengal Basin including Bangladesh and Bhutan Himalaya for 10% probability of exceedance in 50 years. Representative Hazard Curves generated for the Cities of Srinagar, Amritsar, Kanpur, Chittagong, Itanagar and Thimphu have also been depicted in the diagram.

3 Site Classification for the Seismogenic Tectonic Ensemble comprising of Kashmir Himalaya, Northwest India, Nepal Himalaya, Indo-Gangetic Foredeep, Bengal Basin including Bangladesh, Darjeeling-Sikkim Himalaya, Northeast India and Bhutan Himalaya

The effective shear wave velocity is a proxy of shallow subsurface soil characteristics thus rendering its spatial distribution an integral aid towards quantifying sediment stiffness in the region based on contrast in acoustic impedance. National Earthquake Hazard Reduction Program, NEHRP (BSSC, 2003) and Uniform Building Code (UBC, 1997) with similar site response have proposed five broad site classes based on effective shear-wave velocity (V_S^{30}) viz. site class A & B with

https://doi.org/10.5194/nhess-2022-66
Preprint. Discussion started: 22 March 2022

Natural Hazards and Earth System Sciences Discussions

V_S^{30}>1500m/s and 760<V_S^{30}≤1500m/s referring to hard rock & rock site conditions respectively, whereas site class C with 360<V_S^{30}≤760m/s corresponds to soft rock, gravels or hard or very stiff soils, while, stiff soils with 180<V_S^{30}≤360m/s designates site class D. Sun et al. (2018), on the other hand, suggested subcategories in site classes C & D, subdividing each into four subclasses as: C1 (V_S^{30}:620-760m/s), C2 (V_S^{30}:520-620m/s), C3 (V_S^{30}:440-520m/s), C4 (V_S^{30}:360-440m/s), D1 (V_S^{30}:320-360m/s), D2 (V_S^{30}: 280-320m/s), D3 (V_S^{30}:240-280m/s), and D4 (V_S^{30}:180-240m/s) respectively. In both the nomenclatures soft clay with properties like V_S^{30}≤180m/s, moisture content ≥40%, plasticity index >20, and average undrained shear strength <25kPa is classified as site class E, wherein similar but liquefiable soils are categorized under site class F.

https://doi.org/10.5194/nhess-2022-66
Preprint. Discussion started: 22 March 2022


Natural Hazards and Earth System Sciences Discussions

3.1 Regional Site Classification

Shear wave velocity is usually related to the geological characteristics, geomorphic features, elevations, slope gradients and distances from hills/mountains. Thus, the effective shear wave velocity of a region has been estimated for the present Tectonic Ensemble using a multi-polynomial nonlinear regression relationship (Nath et al., 2021a) by combining the attributes like Surface Geology & Geomorphology (GGM), Landform (LF), and Slope (SLP). Thus, a regional site classification map for the Seismogenic Tectonic Ensemble comprising of eight Seismogenic Tectonic Provinces viz. Kashmir Himalaya, Northwest India, Nepal Himalaya, Indo-Gangetic Foredeep, Bengal Basin including Bangladesh, Darjeeling-Sikkim Himalaya, Northeast India and Bhutan Himalaya has been made based on these selected terrain attributes in the nonlinearly regressed relationship (Nath et al., 2021a) given by Eq. (1),

$$V_s^{30} = A*\ln(LF) + B*(GGM)^5 + C*(GGM)^4 + D*(GGM)^3 + E*(GGM)^2 + F*(GGM) + G*\ln(SLP) + H \quad (1)$$

Where, the values of co-efficient i.e. A, B, C, D, E, F, G and H are assigned as 28.887, 0.174, -4.881, 48.668, -201.934, 347.873, 173.646 and -34.572 respectively corresponding to the attributes such as LF, GGM and SLP which refer to Landform, Integrated Geology & Geomorphology and Slope respectively.

3.2 Data: Geophysical and Geotechnical Investigation

The entire Seismogenic Tectonic Ensemble has been extensively explored using both non-invasive techniques such as Ambient Noise Survey and Multi-channel Analysis of Surface Waves (MASW) and invasive techniques such as Downhole Seismic Survey and Geotechnical investigations that include Standard Penetration Test, Atterberg limits test, bulk density test, moisture test, grain size analysis etc. to assess the nature, thickness and sequence of subsurface layers along with estimating related engineering properties to quantify the soil composition, strength, density, water content and other parameters.

3.2.1 Geotechnical Investigation

Standard Penetration Test (SPT) offers a simple but widely applicable tool to determine Geotechnical parameters and establishing a precise subsurface model (Skempton, 1986; Kulhawy and Mayne, 1990) thus becoming most useful among other in-situ field tests for site characterisation of an earthquake county. Hence, boreholes of 0.15m diameter have been drilled with hydraulic feed rotary drilling technique using bentonite circulation following IS 1892 (1979) because of its utility in all the soil type conditions. Several in-situ field tests & laboratory tests have been conducted on the collected soil/sediment samples of each stratum encountered during drilling upto a depth of 30m below the surface level in accordance with IS 2720-1 (1983) for Atterberg limit test, Bulk density & Natural Moisture content, Grain size analysis, and so on throughout the entire Seismogenic Tectonic Ensemble One representative data from each of the six Seismogenic Tectonic

https://doi.org/10.5194/nhess-2022-66
Preprint. Discussion started: 22 March 2022


Natural Hazards and Earth System Sciences Discussions

Provinces are shown in **Fig. 12 (a - f)**, wherein depth wise corrected SPT-N value, Shear wave velocity, Bulk density, Unit Weight, Plasticity Index and Fine Content have been displayed.

Figure 12 Sample Geotechnical data presenting depth-wise variation in lithology, corrected SPT-N, Shear wave velocity, Unit Weight, Bulk Density, Plasticity Index and Fine Content from representative drill holes at (**a**) Srinagar in Kashmir, (**b**) Chandigarh in Punjab, (**c**) Kanpur in Uttar Pradesh, (**d**) Chittagong in Bangladesh, (**e**) Gangtok in Sikkim and (**f**) Itanagar in Arunachal Pradesh.

3.2.2 Geophysical Investigation: Microtremor data acquisition and measurement

Non-invasive Geophysical explorations, characterized by fast data acquisition rate and cost-effectiveness ascertain high-resolution shallow subsurface attributes with the aim of interpreting them in terms of subsurface geology. These tests have, therefore, become popular in providing an effective means of addressing the identified data gaps. Site effect characterization can primarily be carried out by estimating local S-wave velocity profile with depth and by estimating the resonance frequency of the soil/ alluvium column. In this study, Ambient Noise/Microtremor Survey has been conducted to estimate predominant frequency associated with each site while Spectral Analysis of Surface Wave (SASW) & Multi-Channel Analysis of Surface Wave (MASW) Survey have been conducted in the Tectonic Ensemble to generate 2D shear wave velocity tomograms (Park et al., 1999). Resonance frequency that causes ground motion amplification due to the local stratigraphic effect is determined by processing and inverting the spectral ratio of horizontal & vertical components (HVSR) using the Nakamura technique (Nakamura, 2000). Representative Mean Nakamura Ratio and Synthesized 1D Shear Wave Velocity (m/s) obtained by inverting mean H/V spectral ratio in Agartala City is shown in **Fig. 13.**

Figure 13 (**a**) Mean Nakamura Ratio computed from several Microtremor Survey conducted in the City of Agartala at various times of the day and (**b**) Inverted 1D Shear Wave velocity (in m/s) as obtained through inversion of the mean data-driven H/V curve.

3.2.3 SASW and MASW data acquisition and measurement

The Spectral Analysis of Surface Wave (SASW) method provides an estimation of shear wave velocity of the subsurface sediment layers by using the dispersion properties of Rayleigh waves in a multi-layered medium. An impulsive source generates Rayleigh waves, which are detected by geophones. The recorded data is then analyzed in the frequency domain to produce a dispersion curve, which is then inverted (Xia et al., 1999) to compute a depth-dependent shear wave velocity profile. An expanding receiver spread is used to prevent the near-field effects caused by Rayleigh waves and the source-receiver system.

In the recent years, the Multichannel Analysis of Surface Waves (MASW) technique has been implemented for shallow depth engineering studies to obtain the shear wave velocity (V_S). The dispersive property of Rayleigh wave is used to measure subsoil shear wave velocity, which is a function of the rigidity of the medium in which they travel. Data has been

https://doi.org/10.5194/nhess-2022-66
Preprint. Discussion started: 22 March 2022


Natural Hazards and Earth System Sciences Discussions

collected in the field through forward, center, and/or reverse shots. While evaluating the results, we first obtained the fundamental mode phase velocity from surface wave records and then 1D shear wave velocity along depth sections is calculated using the damped least squares inversion process.

The SASW dispersion analysis method is based on phase shift as a function of frequency between two receivers while the MASW depends on phase angles and source to receiver-offset relationship. Representative 1D shear wave velocity along with their corresponding dispersion curves and Joint fit of dispersion curves obtained from SASW survey and H/V curve from Ambient Noise survey at Imphal in Manipur is shown in **Fig. 14.**

Figure 14 (**a**) Representative Ambient Noise driven H/V curve at Imphal in Manipur, (**b**) dispersion curves derived from SASW survey carried out in Imphal, Manipur and (**c**) 1D Shear wave velocity section of the subsurface for the City of Imphal in Manipur obtained from joint inversion of mean HVSR curve of diagram (**a**) and dispersion curve of diagram (**b**).

One of the efficient ways of evaluating shear wave velocity (V_S) is to generate regressed power relations between V_S and SPT-N values. Nath et al. (2021a) worked out depth-dependent site and lithology-specific empirical relationships between SPT-N and V_S for the alluvial-filled terrain of Bengal Basin, Indo-Gangetic Foredeep region, Brahmaputra Valley and Northwest India, which have been extensively used in the present investigation.

The Site Classification map of the entire Seismogenic Tectonic Ensemble comprising of Kashmir Himalaya to Northeast India has been generated by combining topographic slope-based V_S in high elevated areas, nonlinear regression analysis based V_S in low to mid-elevated areas and site specific V_S determination viz. 1D V_S profiles at other locations obtained from Geotechnical borehole sites, MASW sites and microtremor survey sites comprising the alluvium and valleys, considering both the NEHRP and Sun et al. (2018) nomenclature. The enriched database obtained from both invasive and non-invasive investigations and other geoscience attributes like Geology, Geomorphology, Slope and Landform have yielded shear wave velocity categorizing the entire Ensemble region into Site Classes F/E, D4, D3, D2, D1, C4, C3, C2, C1, B and A as shown in **Fig. 15.**

Figure 15 Site Classification map of the Seismogenic Tectonic Ensemble following the nomenclature of Sun et al. (2018) depicting the dominance of site class A, B, C1, C2, and C3 mostly in the hilly terrains of Kashmir Himalaya, Northwest India, Nepal Himalaya, Darjeeling-Sikkim Himalaya, Northeast India and Bhutan Himalaya, while site class C4 and D1 are predominantly seen in the plateau region of western part of Bengal Basin and Shillong Plateau of Northeast India, whereas, D2, D3, D4 and E/F are seen in the alluvial plains of Northwest India, Indo-Gangetic Foredeep, Bengal Basin and Brahmaputra Valley of Northeast India. The topographic gradient based site classification map of India and its surrounding region following Nath et al. (2013) is given in the inset of this diagram.

4 Strong Ground Motion Simulations

https://doi.org/10.5194/nhess-2022-66
Preprint. Discussion started: 22 March 2022


Natural Hazards and Earth System Sciences Discussions

Strong ground motion caused by an earthquake is vital from both seismological and engineering standpoint, as it is required to understand the complexity of the fault system, the rupture process and propagation phenomenon of the near-field seismic waves. The stochastic approach of synthesizing strong ground motion is based on the fact that near-field high frequency ground motion triggered by an earthquake can be formulated by a finite duration white Gaussian noise band constrained by the corner frequency f_o and the peak frequency f_{max}. The simulated acceleration spectrum $A(\omega)$ of shear waves at a distance R from the fault rupture with the seismic moment M_o using stochastic method are theorized in Boore (1983). This method has further been extended to consider major faults termed as finite fault stochastic modelling (Motazedian and Atkinson, 2005). The rupture plane of the finite fault is sub-divided into sub-faults, each of which is referred as point source and the contribution of each fault is added up. The source parameters for ground motion simulation using EXSIM (Boore, 2009; Motazedian and Atkinson, 2005; Atkinson and Assatourians, 2015) package have been taken from GCMT catalogue and various other published literatures. Representative synthetic strong ground motion at Kupwara in Jammu and Kashmir for 2005 Kashmir earthquake of M_w 7.6, Amritsar in Punjab for 1905 Kangra earthquake of M_w 7.8, Patna in Bihar for 1988 Nepal-Bihar earthquake of M_w 6.9, Siliguri in West Bengal for 1934 Bihar-Nepal earthquake of M_w 8.1, Gangtok in Sikkim for 2011 Sikkim earthquake of M_w 6.9 and Hayuliang in Arunachal Pradesh for 1950 Assam earthquake of M_w 8.7 at engineering bedrock level have been presented in **Fig. 16**.

Figure 16 Synthesized strong ground motion at engineering bedrock level using EXSIM software of Boore (2009) at (**a**) Kupwara in Jammu and Kashmir for 2005 Kashmir earthquake of M_w 7.6, (**b**) Amritsar in Punjab for 1905 Kangra earthquake of M_w 7.8, (**c**) Patna in Bihar for 1988 Nepal-Bihar earthquake of M_w 6.9, (**d**) Siliguri in West Bengal for 1934 Bihar-Nepal earthquake of M_w 8.1, (**e**) Gangtok in Sikkim for 2011 Sikkim earthquake of M_w 6.9 and (**f**) Hayuliang in Arunachal Pradesh for 1950 Assam earthquake of M_w 8.7.

5 Site Response Analysis: 1D Nonlinear/Equivalent linear Analysis for Engineering Soil Response Characteristics using DEEPSOIL software package & Surface-consistent PSHA of the Seismogenic Tectonic Ensemble

The nonlinear characteristics of the soil column give rise to the ground motion amplification at surface which is vital in defining the seismic site characterization of a region. Thus, the estimation of site amplification factor for a location situated over soft sediments is responsible for alteration in ground motion at the surface with that at the engineering bedrock. 1D nonlinear/equivalent linear site response analysis suggested by Idriss and Seed (1968) has been followed in the present study and employed through DEEPSOIL analysis package by Hashash et al. (2020) which requires the Geotechnical parameters viz. soil type, thickness of the layer, unit weight and shear wave velocity of the material together with the acceleration time history at engineering bedrock level as input with the assumptions that each soil layer is horizontal, homogeneous, ground surface is leveled, the soil/alluvial column extends to infinity and the incident earthquake motions propagate vertically. Entrapment of seismic waves is the basic phenomenon liable for the ground motion amplification in

https://doi.org/10.5194/nhess-2022-66
Preprint. Discussion started: 22 March 2022


Natural Hazards and Earth System Sciences Discussions

soft sediments. This is caused due to the impedance contrast that exists between the sediments and the bedrock. In nonlinear/equivalent linear site response assessment, the nonlinear effect of the soil/sediment is approximated by updating the linear elastic properties of the soil in accordance with the induced strain level in which the strain compatible shear modulus and damping ratios produce the transfer function for each soil layer. The computation of transfer functions is the key tool in ground response analysis. The function delivers the amplification/de-amplification factor corresponding to the bedrock motion, which is used as an input to get the surface level motion. The response spectrum at the interface between the two layers is estimated as the product of the Fourier amplitude spectrum of the input motion & the transfer function in its spectral form. The workflow underlying the DEEPSOIL Software Package is provided in Nath et al. (2021a).

The present study has used synthesized strong ground motion at engineering bedrock level using EXSIM software for the earthquakes which have major impact on the study region viz. 1905 Kangra earthquake of M_w 7.8, 2005 Kashmir earthquake of M_w 7.6, 1991 Uttarkashi earthquake of M_w 6.8, 1999 Chamoli earthquake of M_w 6.6, 1945 Chamba earthquake of M_w 6.4 for Kashmir Himalaya Tectonic Province Z-VIII and Northwest India Tectonic Province Z- IX; 1934 Bihar-Nepal earthquake of M_w 8.1, 1988 Nepal-Bihar earthquake of M_w 6.8 for Nepal Himalaya; 1905 Kangra earthquake of M_w 7.8, 1934 Bihar-Nepal earthquake of M_w 8.1, 1988 Nepal-Bihar earthquake of M_w 6.8, 1991 Uttarkashi earthquake of M_w 6.8, 1999 Chamoli earthquake of M_w 6.6 for Indo-Gangetic Foredeep Tectonic Province Z-II; 1934 Bihar-Nepal earthquake of M_w 8.1, 1918 Srimangal earthquake of M_w 7.6, 1885 Bengal earthquake of M_w 6.8, 1930 Dhubri earthquake of M_w 7.1, 1964 Sagar Island earthquake of M_w 5.4 for Bengal Basin Tectonic Province Z-I including Bangladesh and 1897 Shillong earthquake of M_w 8.1, 1869 Cacher earthquake of M_w 7.6, 1930 Dhubri earthquake of M_w 7.1 for Shillong Zone in Northeast India Tectonic Province Z-XI ; 1950 Great Assam earthquake of M_w 8.6, 1943 Assam earthquake of M_w 7.1 for Mishmi Block Zone in the Northeast India Tectonic Province Z-XI; 1988 Indo-Burma Earthquake of M_w 7.2, 2016 Manipur earthquake of M_w 6.7 for Eastern Boundary Zone in the Northeast India Tectonic Province Z-XI; 2009 Bhutan earthquake of M_w 6.1, 2011 Sikkim Earthquake of M_w 6.9 for Eastern Himalayan Zone in the Northeast India Tectonic Province Z-XI, Bhutan Himalaya and Darjeeling-Sikkim Himalaya Tectonic Province Z-X by adopting the source parameters from various published literatures with an initial consideration of 5% damping for all soil types to conduct nonlinear/equivalent linear analysis using the DEEPSOIL software package. The amplification spectra is acquired for at least four earthquakes at each of the approximately 20,000 sites in this Tectonic Ensemble region further to achieve the mean site response spectrum as well as the PGA absolute amplification factor at zero time period at each of these sites which exhibit its variation from about 1.25-6.0. Both PGA absolute amplification and spectral amplification is directly related to shear wave velocity ranges, higher ground motion amplification exhibited in site classes F/E, followed by D4 to D1. The firm rock conditions of site classes A & B followed by C1 to C4 show low to moderate absolute and spectral amplification in ground motion seen mostly in the elevated rugged terrains in Kashmir Himalaya, Northwest India, Nepal Himalaya, Indo-Gangetic Foredeep, Darjeeling-Sikkim Himalaya, Northeast India and Bhutan Himalaya. The Spectral Site Amplification Factor (SAF) at a predominant frequency attained by considering both the aforesaid near- and far-field earthquakes for the sites located in Site Classes F/E, D4, D3, D2, D1, C4, C3, C2, C1, B and A are having spectral amplifications of 5.8, 4.8, 4.2, 3.9, 3.3, 2.58, 2.2, 1.87, 1.81,

https://doi.org/10.5194/nhess-2022-66
Preprint. Discussion started: 22 March 2022


Natural Hazards and Earth System Sciences Discussions

1.4 and 1.0 respectively at the predominant frequency range of 0.73 to 8.5 Hz as envisaged through nonlinear soil-structure interaction modelling. The Surface-consistent Probabilistic Seismic Hazard in terms of PGA and PSA estimated by convolving absolute and spectral site amplifications with the bedrock PGA and PSA with the former being presented in **Fig. 17** along with Generic Site Response Curves and representative maximum occurring site parameters viz. Predominant Frequency, both Absolute and Spectral Amplification Factors, PSA at 1.0sec, 0.3sec and 0.2sec periods focussing mostly on the disastrous locations in site classes E/F or D4 in each Seismogenic Tectonic Province of the ensemble especially in the city of Srinagar located in the Tectonic Province of Kashmir Himalaya depicting surface PGA of 1.15g, Amritsar in the Northwest Tectonic Province with surface PGA of 0.40g, Agra in the Indo-Gangetic Tectonic Province with surface PGA of 0.35g, Kolkata in the Bengal Basin Tectonic Province with surface PGA of 0.39g, Dhaka in the Bengal Basin Tectonic Province with surface PGA of 0.40g, Guwahati with surface PGA of 1.9g, Aizawl with surface PGA of 0.54g, Imphal with surface PGA of 0.83g, Agartala with surface PGA of 0.39g, Shillong with surface PGA of 0.76g, Itanagar with surface PGA of 0.57g, Kohima with surface PGA of 0.88g all located in the most seismogenic Northeast India Tectonic Province Thimphu lying in the seismogenic Bhutan Himalaya with surface PGA of 0.41g and Gangtok located in the Darjeeling-Sikkim Himalaya Tectonic Province with surface PGA of 0.60g for 475 years of return period, to name a few selected cities and urban centres that were reported to have been impacted by earthquake induced secondary hazards of liquefaction and ground failure as seen in **Fig. 17**. The observations are seen to influence the surface-consistent PGA and PSA significantly with multifold enhancement in the design response spectra of the ensemble as shown in **Fig. 18.**

Figure 17 Surface-consistent Probabilistic Seismic Hazard of the Seismogenic Tectonic Ensemble comprising of Kashmir Himalaya to Northeast India covering the entire stretch of Northwest India, Nepal Himalaya, Indo-Gangetic Foredeep, Bengal Basin containing both West Bengal and Bangladesh, Darjeeling-Sikkim Himalaya and Bhutan Himalaya for 10% probability of exceedance in 50 years. Generic site response curves (red bold line) ±1 Standard Deviation (red dotted lines) and associated site parameters mostly in the site class E/F/D4 in each Seismogenic Tectonic Province are also presented in the diagram.

https://doi.org/10.5194/nhess-2022-66
Preprint. Discussion started: 22 March 2022


Natural Hazards and Earth System Sciences Discussions

The 5% damped design response spectra generated following the International Building Code (IBC, 2009) for the PSA at 1.0sec and 0.2sec with 10% probability of exceedance in 50 years for 10 selected representative landmarks taken from Kashmir Himalaya, Northwest India, Indo-Gangetic Foredeep region, Bengal Basin including Bangladesh, Northeast India and Bhutan Himalaya at both the bedrock and surface level are presented in **Fig. 18**, which display an appreciable enhancement in the design response values.

Figure 18 Representative Design response spectra (5% damped) worked out at both engineering bedrock and surface-consistent level using PSA at 1.0sec and 0.2sec with 10% probability of exceedance in 50 years are shown for the city of (**a**) Srinagar in Jammu and Kashmir, (**b**) Chandigarh in Punjab, (c) Gurugram in Haryana, (**d**) Kanpur in Uttar Pradesh, (**e**) Asansol in West Bengal, (**f**) Chittagong in Bangladesh, (**g**) Shillong in Meghalaya, (**h**) Imphal in Manipur, (**i**) Itanagar in Arunachal Pradesh and (**j**) Thimphu in Bhutan.

6 Structural Impact Assessment in terms of Damage Potential Modelling and Human Casualty Assessment in some selected cities in the seismogenic Tectonic Ensemble from Kashmir Himalaya to Northeast India

To speculate the damage probability, elaborate information such as number of buildings, building footprint, built-up area, soil map, earthquake sources, empirical ground motion prediction relationships, cost schedules of different model building types and capacity & fragility functions are the most essential components of the well-known SELENA package**.** The algorithm for damage potential estimation is demonstrated in Molina et al. (2014) while Nath et al. (2015, 2021a) & Ghatak et al. (2017) have picturized its flow diagram, which has been followed in this study as well. Human casualty, additionally, has been predicted based on the seismic hazard condition at surface level and population distribution of the Cities in accordance with the Census data (Chandramouli and General, 2011) and various authentic internet sources available on the web. Number of casualties has been calculated in terms of four different levels of injuries at three significant times of the day viz. night time (at 02:00 AM), day time (at 10:00 AM) and commuting time (at 05:00 PM) scenarios respectively considering the occupancy classes. This methodology gives the number of human casualties due to building collapse owing to ground shaking where the percentage indoor and outdoor population for a specific time of the day is taken from Molina et al. (2010) and illustrated in **Table 1.**

Table 1: Percentage of indoor and outdoor population dependent on the time of the day (Molina et al., 2010; Nath et al., 2015; Ghatak et al., 2017)

6.1 Structural Damage Assessment through Capacity Spectrum Method

The basic principle governing the SELENA is the Capacity Spectrum Method (Molina and Lindholm, 2005; Molina et al., 2010) where the building specific capacity curve (Molina et al., 2010) is compared with response spectra from the input ground motion. The damage probability in each of the 5000 sample geo-units selected in each city and urban centers in all

https://doi.org/10.5194/nhess-2022-66
Preprint. Discussion started: 22 March 2022


Natural Hazards and Earth System Sciences Discussions

the Tectonic Provinces in the entire Tectonic Ensemble has been estimated from the given ground motion relationship; which comprises of Capacity Spectrum selection, Demand Spectrum generation and Performance Point calculation. Design, Yield and Ultimate Capacity are the three control points of the building capacity curve. The building capacity curve is supposed to act elastically linearly up to the yield point, then changes its state to plastic from the yield point to the ultimate point, and finally behaving completely plastic when it exceeds the ultimate point. The peak building response is computed using the demand spectrum curve from spectral displacements at 0.3s and 1.0s period. The intersection of the building capacity and seismic demand curves is defined as the Performance Point. Vulnerability or fragility curves for four damage states are required for the estimation of damage probabilities, which are calculated in terms of lognormal probability distribution of damage from the selected capacity curve as formulated in Molina et al. (2014). The obtained displacement from Performance Point is then superimposed over the fragility curves to compute the damage probability in each of the various damage states, namely "None," "Slight," "Moderate," "Extensive," and "Complete". Capacity and Fragility characteristics used in this study have been adopted from NIBS (2002), whereas, the nomenclature of model building types are adhered to FEMA (2000) and WHE-PAGER (2008). The number of casualties considering direct structural damage for any given model building type from all 5000 sample Geounits, level of building damage, and injury severity can be calculated by Coburn and Spence (2002) and Molina et al. (2010).

In the city of Srinagar in the Kashmir Himalaya Seismogenic Tectonic Province, 92-100% of all the eleven model building types viz. A1, RS2, URML, URMM, C1L, C1M, C1H, C3L, C3M, C3H and HER, may experience ‘complete’ damage. Most of the RS2, URML, C3M and HER type buildings may suffer from ‘complete’ damage and other building types may undergo ‘extensive’ to ‘complete’ damage state in Chandigarh in the Northwest India Tectonic Province, whereas, in Gurugram in Haryana the buildings are mostly of reinforced concrete types, out of which 32-44% are supposed to face ‘moderate’ to ‘complete’ damage state. Kanpur, one of the major financial and industrial centres of Indo-Gangetic Foredeep Tectonic region, has 11 types of model buildings and 85-95% of A1, RS2, URML and URMM types, which all are susceptible to ‘complete’ damage state. In Asansol from the western part of the Bengal Basin Tectonic Province, both kinds of ductile and non-ductile reinforced concrete buildings are found mostly in the safer state, while, 57-100% of all the building types are expected to undergo ‘complete’ damage in the Port City of Chittagong from the eastern part of the Bengal Basin. Northeast India on the other hand presents a disastrous scenario so far as earthquake induced structural damage is concerned since 60-100% of all the building types existing in the cities of Shillong and Imphal may face ‘complete’ damage. In Itanagar, A1, RS2 and URML types of buildings are vulnerable to ‘complete’ damage state, whereas, RS2, URML, C1L, C1M, C1H, C3L and C3M types of buildings will probably experience ‘extensive’ to ‘complete’ damage states in Thimphu. The probabilities of each damage state for the model building types found in the cities of Srinagar, Chandigarh, Gurugram, Kanpur, Asansol, Chittagong, Thimphu, Shillong, Imphal and Itanagar have been presented in **Fig. 19** in the form of bar graphs by considering the surface consistent probabilistic seismic hazard for 10% probability of exceedance in 50 years**.**

https://doi.org/10.5194/nhess-2022-66
Preprint. Discussion started: 22 March 2022


Natural Hazards and Earth System Sciences Discussions

Figure 19 Representative Discrete damage probability estimated using SELENA–based Capacity Spectrum Method (Molina and Lindholm, 2005; Molina et al., 2010) in terms of "None", "Slight", "Moderate", "Extensive", and "Complete" for the model building types viz. A1, RS2, URML, URMM, C1L, C1M, C1H, C3L, C3M, C3H and HER (FEMA, 2000; WHE-PAGER, 2008) are shown for (**a**) Srinagar in Jammu and Kashmir, (**b**) Chandigarh in Punjab, (**c**) Gurugram in Haryana, (**d**) Kanpur in Uttar Pradesh, (**e**) Asansol in West Bengal, (**f**) Chittagong in Bangladesh, (**g**) Thimphu in Bhutan, (**h**) Shillong in Meghalaya, (**i**) Imphal in Manipur and (**j**) Itanagar in Arunachal Pradesh for the surface-consistent probabilistic seismic hazard for 10% probability of exceedance in 50years.

Thereafter, human inventory data are used in SELENA to predict the number of persons facing different casualty/injury levels viz. "Low", "Medium", "Heavy" and "Death" for three distinct times of the day i.e. "Day time (10:00 AM)", "commuting time (5:00 PM)" and "night time (2:00 AM)" as shown in **Fig. 20** when exposed to probabilistic seismic hazard condition for 10% probability of exceedance in 50 years at surface level. The human fatality index of the selected Cities of the study Tectonic Ensemble is enlisted in **Table 2**.

Table 2. Representation of Fatality index in Srinagar, Chandigarh, Gurugram, Kanpur, Asansol, Chittagong, Thimphu, Shillong, Imphal and Itanagar.

Figure 20 Number of Human Casualties at different levels of injury in three different times of the day for (**a**) Srinagar in Jammu and Kashmir, (**b**) Chandigarh in Punjab, (**c**) Gurugram in Haryana, (**d**) Kanpur in Uttar Pradesh, (**e**) Asansol in West Bengal, (**f**) Chittagong in Bangladesh, (**g**) Thimphu in Bhutan, (**h**) Shillong in Meghalaya, (**j**) Imphal in Manipur and (**h**) Itanagar in Arunachal Pradesh for the surface-consistent probabilistic seismic hazard for 10% probability of exceedance in 50years.

7 Conclusions

The vulnerability of the modern society towards earthquake hazard is increasing with time. Although the occurrence of earthquakes is inevitable, the reduction of the social and economic setback during earthquakes can be achieved through a comprehensive assessment of surface-consistent seismic hazard, vulnerability, risk and structural impact studies. 59% of the total land-cover of India that comprise of three morphotectonic provinces is susceptible to seismic hazard. The fatalities in the urban agglomerations due to future great Himalayan earthquakes have been predicted to be around 150 and 200 thousand. Therefore, as far as the seismic hazard in the country is concerned, the present situation is rather alarming. In the present investigation, rigorous formulations of hazard components have been adopted to deliver a case for surface consistent Probabilistic Seismic Hazard through detailed site characterization of this Himalayan and Sub-Himalayan Tectonic Ensemble comprising of Kashmir Himalaya to Northeast India including SELENA-based urban structural impact assessment for all the Capital-Spiritual-Commercial Cities of this Ensemble thus bringing in an unique benchmark like regional-local

https://doi.org/10.5194/nhess-2022-66
Preprint. Discussion started: 22 March 2022

hybrid seismic hazard-disaster model for pre-disaster preparedness in the form of updated urban by-laws and post-disaster rehabilitation and future disaster management.

Ethics declarations

We consciously assure that the manuscript contains our own original work, which has not been previously published elsewhere. The paper reflects our own research and analysis in a truthful and complete manner.

Availability of data and material: Data that support the findings in this study are available from our own extensive field work.

Author Contributions: SKN, AS, JM and AB took part in conceptualization, methodology, analysis, investigation, validation, writing-original draft preparation. CG involved in characterizing Bengal Basin & Indo-Gangetic Foredeep region. ASG involved in Risk map & Selena input preparation and map composition. PS involved in Selena input generation and diagram preparation. SB involved in Selena based Damage Modelling.

Competing Interest: The authors declare that they have no conflicts of interest.

References

Adhikari, M. D. and Nath, S. K.: Site-specific next generation ground motion prediction models for Darjeeling-Sikkim Himalaya using strong motion seismometry, Journal of Indian Geophysical Union, 20(2), 151-170, 2016.

Atkinson, G. M. and Assatourians, K.: Implementation and Validation of EXSIM (A Stochastic Finite-Fault Ground-Motion Simulation Algorithm) on the SCEC Broadband Platform, Seismological Research Letter, 86, 1, https://doi.org/10.1785/0220140097, 2015.

Boore, D. M.: Stochastic simulation of high-frequency ground motions based on seismological models of the radiated spectra, Bulletin of the Seismological Society of America, https://doi.org/10.1785/BSSA07306A1865, 79, 1865-1894, 1983.

Boore, D. M.: Comparing stochastic point-source and finite-source ground-motion simulations: SMSIM and EXSIM. Bulletin of the Seismological Society of America, 99(6), 3202-3216, https://doi.org/10.1785/0120090056, 2009.

BMTPC: Vulnerability Atlas of India: Earthquake, Wind, Flood, Landslide, Thunderstorm Maps and Damaged Risk to Housing, Building Materials and Technology Promotion council, Ministry of Housing & Urban Affairs, Government of India, third edition, available at: https://vai.bmtpc.org/, 2019.

BSSC: NEHRP recommended provisions for seismic regulations for new buildings and other structures, 2003 Edition, Part 1: Provisions, Building Seismic Safety Council for the Federal Emergency Management Agency (Report FEMA 450), and Washington D.C., available at: https://www.nehrp.gov/, 2003.

Chandramouli, C. and General, R.: Census of India 2011, Provisional Population Totals, New Delhi: Government of India, 409-413, available at: https://censusindia.gov.in/, 2011.

CIESIN: Center for International Earth Science Information Network, Columbia University supported by United Nations Food and Agriculture Programme and Centro Internacional de Agricultura Tropical, Socioeconomic Data and Applications Center, Columbia University, available at: http://sedac.ciesin.columbia.edu/gpw, Last Accessed February 12, 2010.

Coburn, A. and Spence, R.: Earthquake protection, second edition, John Wiley & Sons Limited, 2002.

Cornell, C. A.: Engineering Seismic Risk Analysis, Bulletin of Seismological Society of America, 58, 1583–1606, https://doi.org/10.1785/BSSA0580051583, 1968.

Esteva, L.: Seismic Risk and Seismic Design Decisions, In Seismic Design for Nuclear Power Plants, R. J. Hansen (Editor), Massachusetts Institute of Technology Press, Cambridge, MA, USA, 142–82, 1970.

FEMA: Prestandard and commentary for the Seismic Rehabilitation of Buildings, Federal Emergency Management Agency 356, Washington D.C., 2000.

Frankel, A.: Mapping seismic hazard in the central and eastern United States. Seismological Research Letters, 66(4), 8-21, https://doi.org/10.1785/gssrl.66.4.8, 1995.

Ghatak, C., Nath, S. K., and Devaraj, N.: Earthquake Induced Deterministic Damage and Economic Loss Estimation for Kolkata, India, Journal of Rehabilitation in Civil Engineering, 5(2), 01-21, https://doi.org/10.22075/JRCE.2017.3090.1166, 2017.

Grünthal, G. and Wahlström, R.: New generation of probabilistic seismic hazard assessment for the area Cologne/Aachen considering the uncertainties of the input data, Natural Hazards 38,159–176, https://doi.org/10.1007/s11069-005-8611-7, 2006.

Hashash, Y. M. A., Musgrove, M. I., Harmon, J. A., Ilhan, O., Xing, G., Numanoglu, O., Groholski, D. R., Phillips, C. A., and Park, D.: "DEEPSOIL 7, User Manual", Urbana, IL, Board of Trustees of University of Illinois at Urbana-Champaign, available at: http://deepsoil.cee.illinois.edu/, 2020.

IBC: International Building Code, International Code Council, Inc. Country Club Hills, Illinois, 2009.

Idriss, I. M. and Seed, H. B.: Seismic response of horizontal soil layers, Journal of the Soil Mechanics and Foundations Division ASCE, 94 (SM4), 1003-1031, https://doi.org/10.1061/JSFEAQ.0001163, 1968.

IS 1892: Indian Standard code of Practice for subsurface investigation for foundations, Bureau of Indian Standards, New Delhi, 1-45, 1979.

IS 2720-1: Methods of test for soils, Part 1: Preparation of dry soil samples for various tests, Bureau of Indian Standards, New Delhi, 1-10, 1983.

Ishita, R. P. and Khandaker, S.: Application of Analytical Hierarchical Process and GIS in Earthquake Vulnerability Assessment: Case Study of Ward 37 and 69 in Dhaka City, Journal of Bangladesh Institute of Planners, 3, 103-112, available at: https://www.bip.org.bd/, 2010.

Karra, K., Kontgis, C., Statman-Weil, Z., Mazzariello, J. C., Mathis, M., and Brumby, S. P.: Global land use/land cover with Sentinel 2 and deep learning, In: 2021 IEEE International Geoscience and Remote Sensing Symposium IGARSS, IEEE, 4704-4707, https://doi.org/10.1109/IGARSS47720.2021.9553499, 2021.

Karimzadeh, S., Miyajima, M., Hassanzadeh, R., Amiraslanzadeh, R., and Kamel, B.: A GIS-based seismic hazard, building vulnerability and human loss assessment for the earthquake scenario in Tabriz, Soil Dynamics and Earthquake Engineering 66, 263-280, https://doi.org/10.1016/j.soildyn.2014.06.026, 2014.

Kijko, A.: Estimation of the Maximum Earthquake Magnitude, Pure and Applied Geophysics, 161, 1655–1681, https://doi.org/10.1007/s00024-004-2531-4, 2004.

Kijko, A. and Graham, G.: Parametric-historic procedure for probabilistic seismic hazard analysis: Part I - estimation of maximum regional magnitude mmax, Pure and Applied Geophysics, 152, 413-442, https://doi.org/10.1007/s000240050161, 1998.

Kulhawy, F. H. and Mayne, P. W.: Manual on estimating soil properties for foundation design (No. EPRI-EL-6800), Electric Power Research Inst., Palo Alto, CA (USA), Cornell Univ., Ithaca, NY (USA), Geotechnical Engineering Group, 1990.

Maiti, S. K., Nath, S. K., Adhikari, M. D., Srivastava, N., Sengupta, P., and Gupta, A. K.: Probabilistic seismic hazard model of West Bengal, India, Journal of Earthquake Engineering, 21(7), 1113-1157, https://doi.org/10.1080/13632469.2016.1210054, 2017.

McGuire, R. K.: FORTRAN Computer Program for Seismic Risk Analysis, US Geological Survey, 76–67, https://doi.org/10.3133/ofr7667, 1976.

Molina, S. and Lindholm, C.: A logic tree extension of the capacity spectrum method developed to estimate seismic risk in Oslo, Norway, Journal of Earthquake Engineering, 9(06), 877-897, https://doi.org/10.1142/S1363246905002201, 2005.

Molina, S., Lang, D. H., and Lindholm, C. D.: SELENA—an open-source tool for seismic risk and loss assessment using logic tree computation procedure, Computers & Geosciences, 36(3), 257–269, https://doi.org/10.1016/j.cageo.2009.07.006, 2010.

Molina, S., Lang, D. H., and Lindholm, C. D.: SELENA v6.0: User and Technical Manual v6.0, Report no. 14-003, Kjeller (Norway) – Alicante (Spain), 102, 2014.

Motazedian, D. and Atkinson, G. M.: Stochastic finite-fault modeling based on a dynamic corner frequency, Bulletin of the Seismological Society of America, 95, 995-1010, https://doi.org/10.1785/0120030207, 2005.

Nakamura, Y.: Clear identification of fundamental idea of Nakamura's technique and its applications, In: Proceedings of the 12th world conference on earthquake engineering, vol. 2656, New Zealand, Auckland, 2000.

Nath, S. K., Raj, A., Thingbaijam, K. K. S., and Kumar, A.: Ground Motion Synthesis and Seismic Scenario in Guwahati City—A Stochastic Approach, Seismological Research Letters, 80 (2), 233–242, https://doi.org/10.1785/gssrl.80.2.233, 2009.

Nath, S. K. and Thingbaijam, S. K. K.: Probabilistic Seismic Hazard Assessment of India, Seismological Research Letters, 83 (1), 135–149, https://doi.org/10.1785/gssrl.83.1.135, 2012.

Nath, S. K., Thingbaijam, K. K. S., Maiti, S. K., and Nayak, A.: Ground-motion predictions in Shillong region, northeast India, Journal of Seismology, 16(3), 475-48, https://doi.org/10.1007/s10950-012-9285-8, 2012.

https://doi.org/10.5194/nhess-2022-66
Preprint. Discussion started: 22 March 2022

Nath, S. K., Thingbaijam, K. K. S., Adhikari, M. D., Nayak, A., Devaraj, N., Ghosh, S. K., and Mahajan, A. K.: Topographic gradient based site characterization in India complemented by strong ground-motion spectral attributes, Soil Dynamics and Earthquake Engineering, 55, 233-246, https://doi.org/10.1016/j.soildyn.2013.09.005, 2013.

Nath, S. K., Adhikari, M. D., Maiti, S. K., Devaraj, N., Srivastava, N., and Mohapatra, L. D.: Earthquake scenario in West Bengal with emphasis on seismic hazard microzonation of the city of Kolkata, India, Natural Hazards and Earth System Sciences, 14, 2549–2575, https://doi.org/10.5194/nhess-14-2549-2014, 2014.

Nath, S. K., Adhikari, M. D., Devaraj, N., and Maiti, S. K.: Seismic vulnerability and risk assessment of Kolkata City, India, Natural Hazards Earth System Sciences, 15, 1103–1121, https://doi.org/10.5194/nhess-15-1103-2015, 2015.

Nath, S. K., Mandal, S., Adhikari, M. D., and Maiti, S. K.: A Unified Earthquake Catalogue for South Asia covering the period 1900-2014, Natural Hazards, 85(3), 1787-1810, https://doi.org/10.1007/s11069-016-2665-6, 2017.

Nath, S. K.: Probabilistic Seismic Hazard Atlas of 40 Cities in India published by Geoscience Division, Ministry of Earth Sciences (MoES), Govt. of India, New Delhi, © MoES, Govt. of India, 457p, 2017.

Nath, S. K., Adhikari, M. D., Maiti, S. K., and Ghatak, C.: Earthquake hazard potential of Indo-Gangetic Foredeep: its seismotectonism, hazard, and damage modeling for the cities of Patna, Lucknow, and Varanasi, Journal of Seismology, 23, 725–769, https://doi.org/10.1007/s10950-019-09832-3, 2019.

Nath, S. K., Ghatak, C., Sengupta, A., Biswas, A., Madan, J., and Srivastava, A.: Regional–Local Hybrid Seismic Hazard and Disaster Modeling of the Five Tectonic Province Ensemble Consisting of Westcentral Himalaya to Northeast India, In: Sitharam T., Jakka R., Kolathayar S. (eds) Latest Developments in Geotechnical Earthquake Engineering and Soil Dynamics, Springer Transactions in Civil and Environmental Engineering, Springer, Singapore, 14, 307-358, https://doi.org/10.1007/978-981-16-1468-2_14, 2021a.

Nath, S. K., Sengupta, A., and Srivastava, A.: Remote sensing GIS-based landslide susceptibility & risk modeling in Darjeeling–Sikkim Himalaya together with FEM-based slope stability analysis of the terrain, Natural Hazards, 108, 3271–3304, https://doi.org/10.1007/s11069-021-04823-5, 2021b.

NIBS: HAZUS99 - earthquake loss estimation methodology, technical manual, in Technical Manual, pp. 325, FEMA, Federal Emergency Management Agency, National Institute of Building Sciences (NIBS), Washington D.C., 2002.

Panahi, M., Rezaie, F., and Meshkani, S. A.: Seismic vulnerability assessment of school buildings in Tehran city based on AHP and GIS, Natural Hazards and Earth System Sciences, 14, 969–979, https://doi.org/10.5194/nhess-14-969-2014, 2014.

Park, C. B., Miller, R. D., and Xia, J.: Multichannel analysis of surface waves, Geophysics, 64(3), 800-808, https://doi.org/10.1190/1.1444590, 1999.

Reveshti, M. A. and Gharakhlou, M.: Modeling of Urban Building Vulnerability in Earthquake against Using Analytical Hierarchy Process (AHP) and GIS, A case study on Zanjan City, Northwest of Iran, available at: https://www.sid.ir/en/journal/ViewPaper.aspx?id=180752, 2009.

Scherbaum, F., Delavaud, E., and Riggelsen, C.: Model selection in seismic hazard analysis: An information-theoretic perspective, Bulletin of the Seismological Society of America, 99(6), 3234-3247, https://doi.org/10.1785/0120080347, 2009.

605 Skempton, A. W.: Standard penetration test procedures and the effects in sands of overburden pressure, relative density, particle size, ageing and overconsolidation, Geotechnique, 36(3), 425-447, https://doi.org/10.1680/geot.1986.36.3.425, 1986.

Sun, C. G., Kim, H. S., and Cho, H. I.: Geo-Proxy-Based Site Classification for Regional Zonation of Seismic Site Effects in South Korea, Applied Sciences, 8(2), 314, https://doi.org/10.3390/app8020314, 2018.

UBC: Uniform building code: International Conference of Building Officials, Uniform Building Code, Whittier, California,
610 1997.

WHE-PAGER: WHE-PAGER Phase 2, Development of Analytical Seismic Vulnerability Functions, EERI-WHE-US Geological Survey, 2008.

Xia, J., Miller, R. D., and Park, C. B.: Estimation of near-surface shear-wave velocity by inversion of Rayleigh waves, Geophysics, 64(3), 691-700, https://doi.org/10.1190/1.1444578, 1999.

615

620

625

630

https://doi.org/10.5194/nhess-2022-66
Preprint. Discussion started: 22 March 2022

Natural Hazards and Earth System Sciences
Discussions

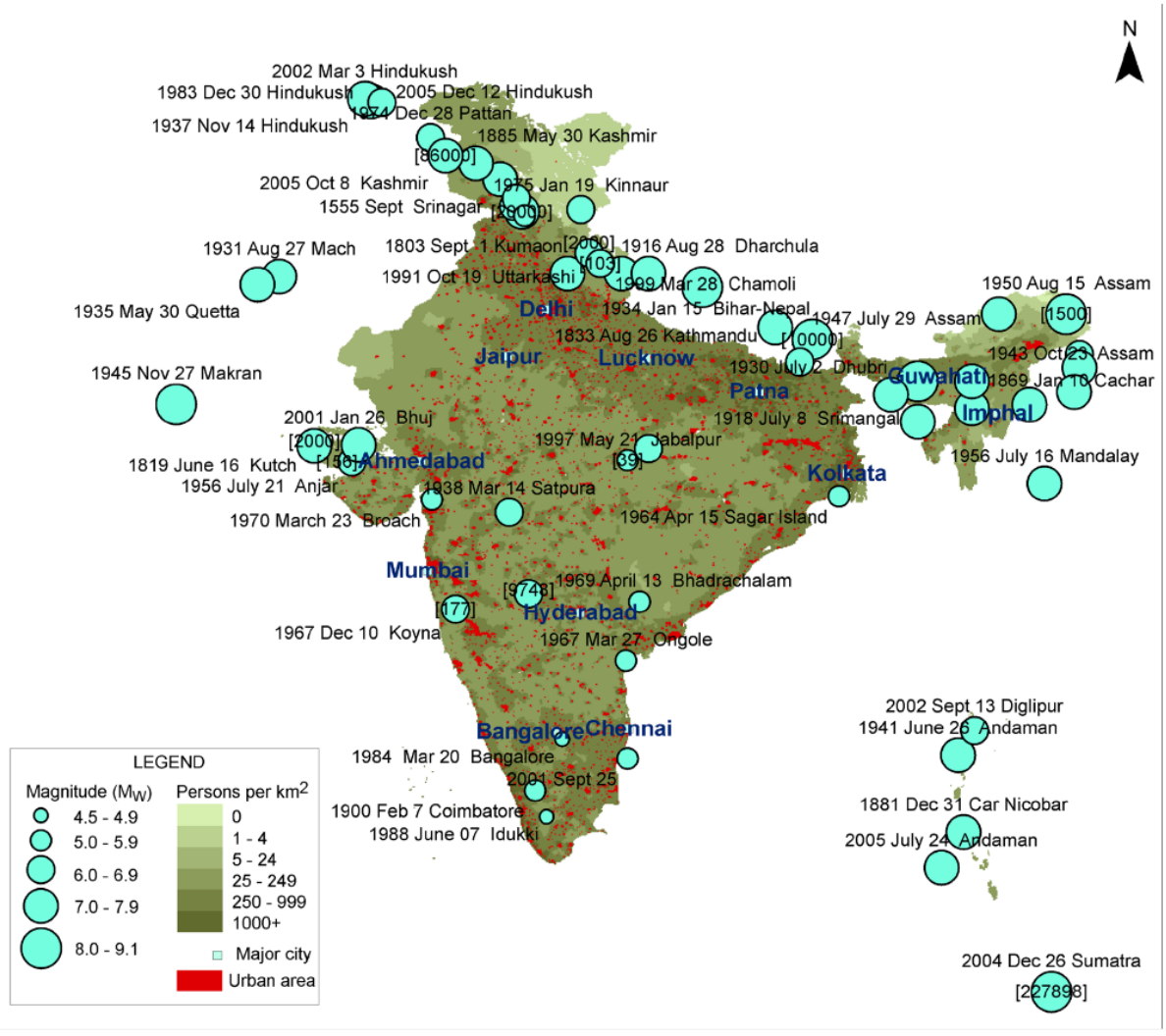

Figure 1 Significant earthquakes in India and its surrounding region illustrated with approximate epicentre locations together with corresponding casualty on the backdrop of population density distribution and urban exposure from the Centre for International Earth Science Information Network (CIESIN, 2010; Nath, 2017) for the year 2005.

https://doi.org/10.5194/nhess-2022-66
Preprint. Discussion started: 22 March 2022

Natural Hazards and Earth System Sciences
Discussions

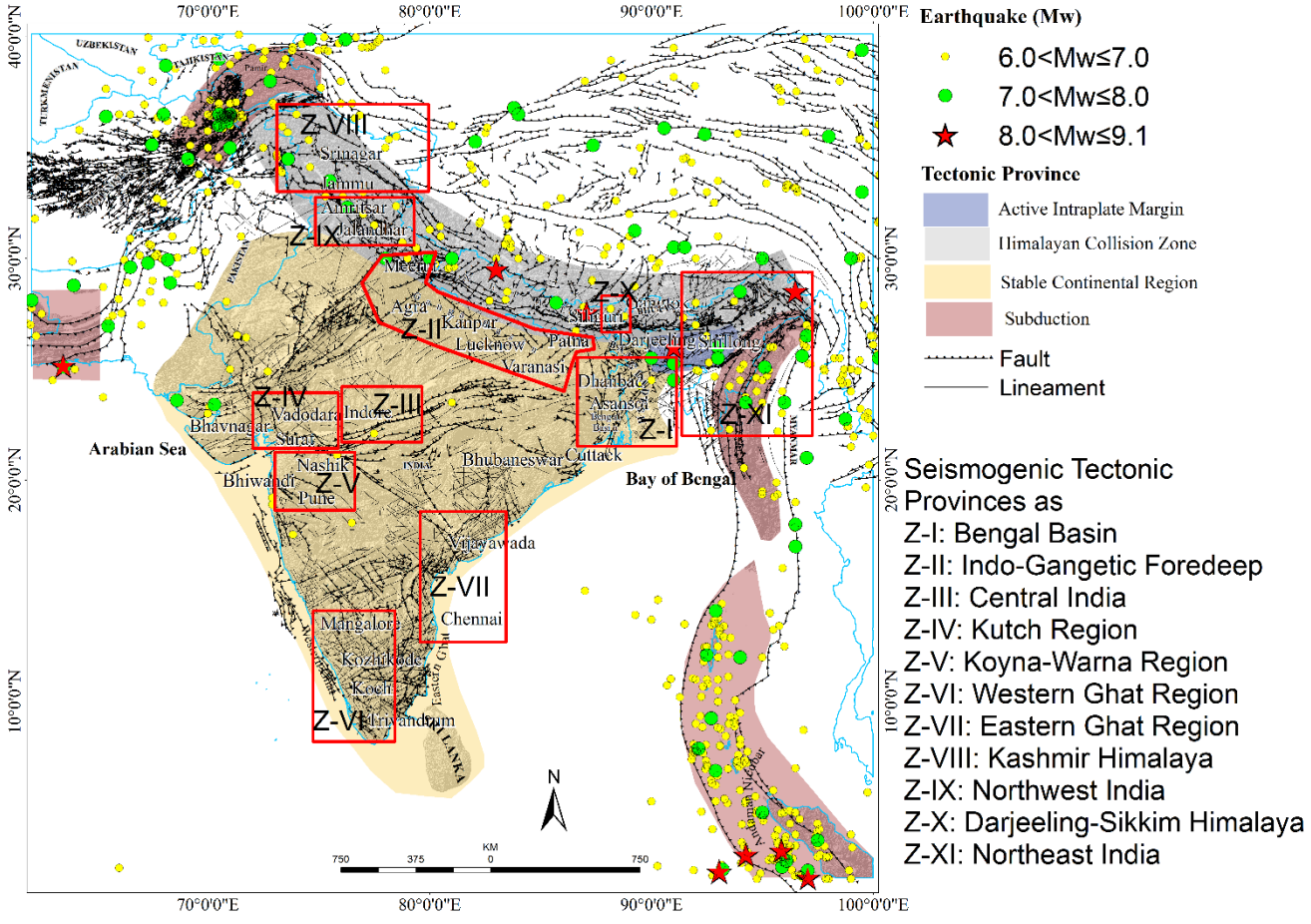

645 **Figure 2** Eleven Major Seismogenic Tectonic Provinces marked as 'Z-I to Z-XI' on the Regional Seismotectonic Map of India (Nath, 2017).

https://doi.org/10.5194/nhess-2022-66
Preprint. Discussion started: 22 March 2022

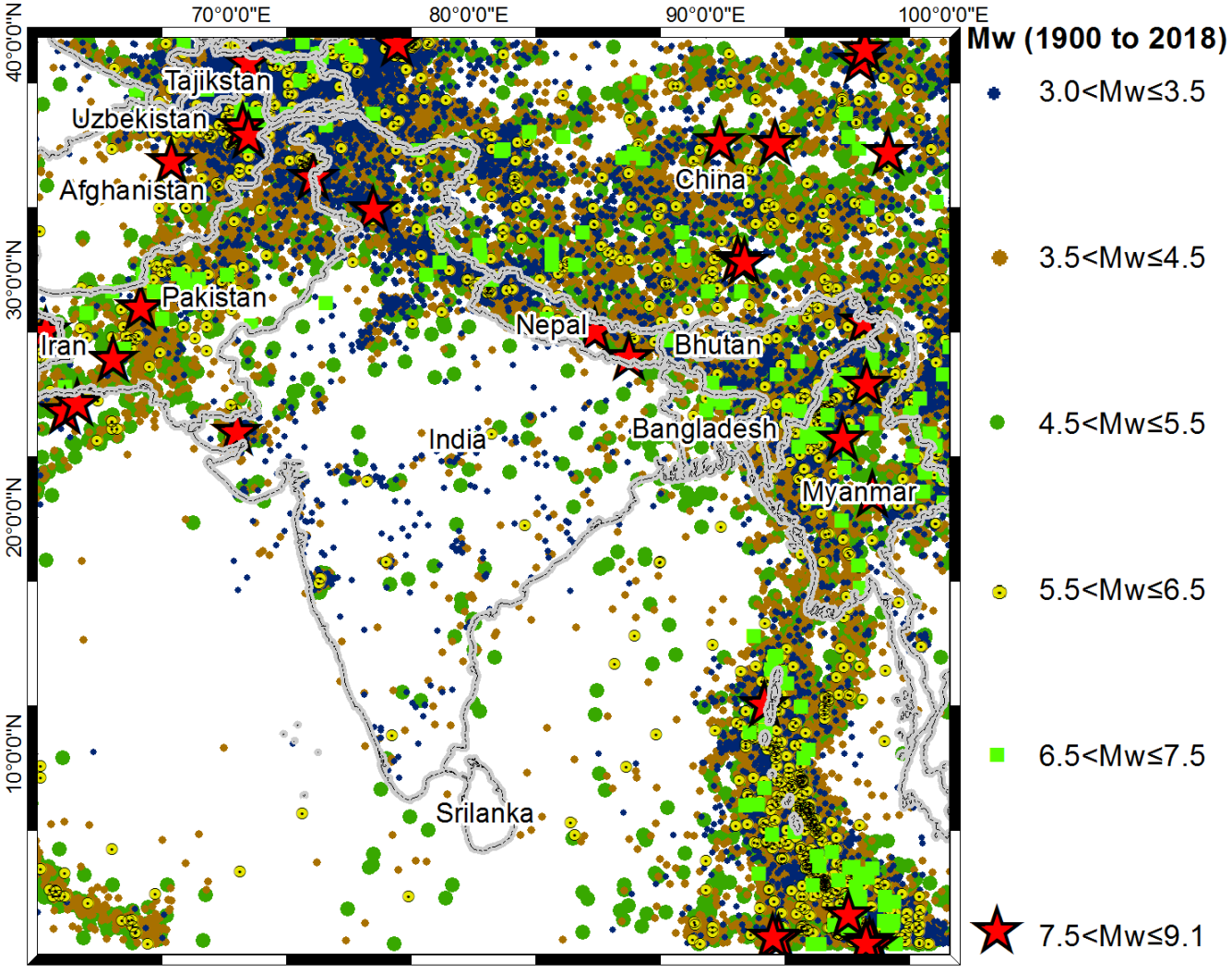

Figure 3 Declustered seismicity map of India and its surrounding region considered from an earthquake catalogue spanning over 1900-2018 depicting 64,153 Mainshock Events (after Nath et al., 2017).

https://doi.org/10.5194/nhess-2022-66
Preprint. Discussion started: 22 March 2022

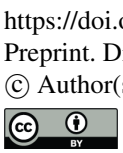

Natural Hazards and Earth System Sciences
Discussions

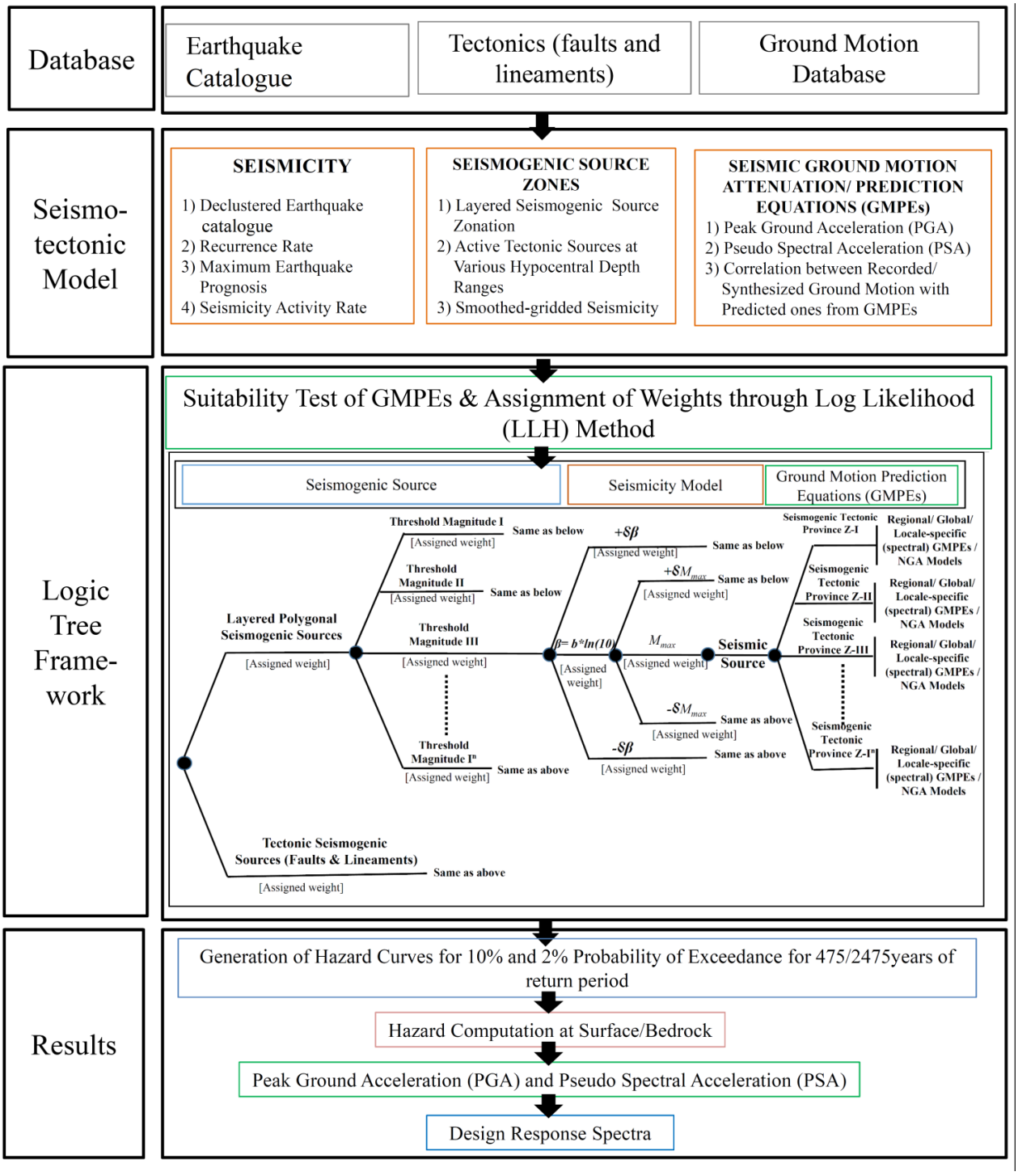

Figure 4 Computational Protocol for Probabilistic Seismic Hazard Assessment of an Earthquake County comprising of several Seismogenic Tectonic Provinces.

https://doi.org/10.5194/nhess-2022-66
Preprint. Discussion started: 22 March 2022

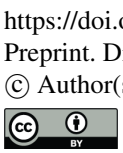

Natural Hazards and Earth System Sciences
Discussions
Open Access
EGU

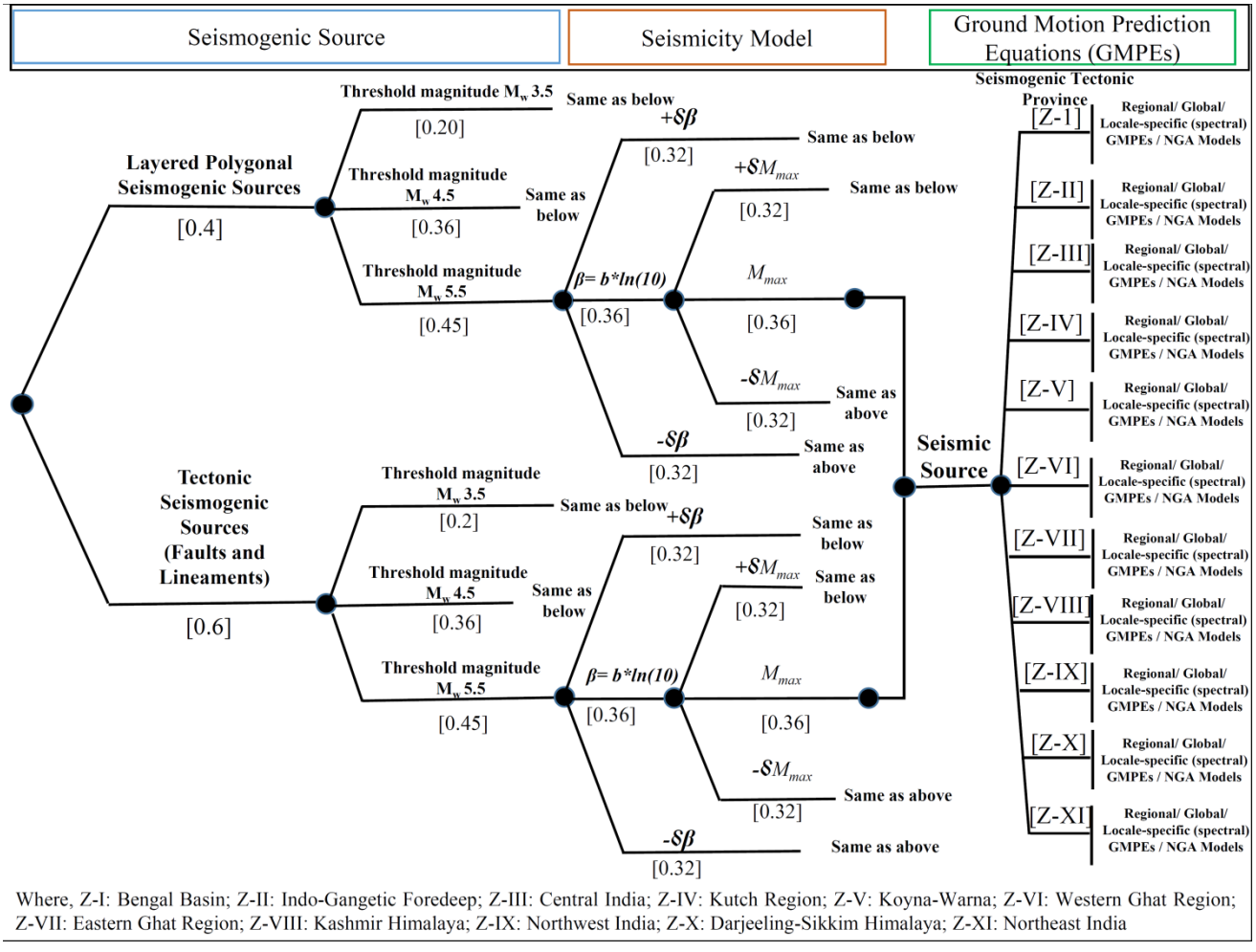

Figure 5 A typical logic tree formulation for computing Probabilistic Seismic Hazard at each node of the Study Region (modified from Nath and Thingbaijam, 2012).

https://doi.org/10.5194/nhess-2022-66
Preprint. Discussion started: 22 March 2022

Natural Hazards and Earth System Sciences
Discussions

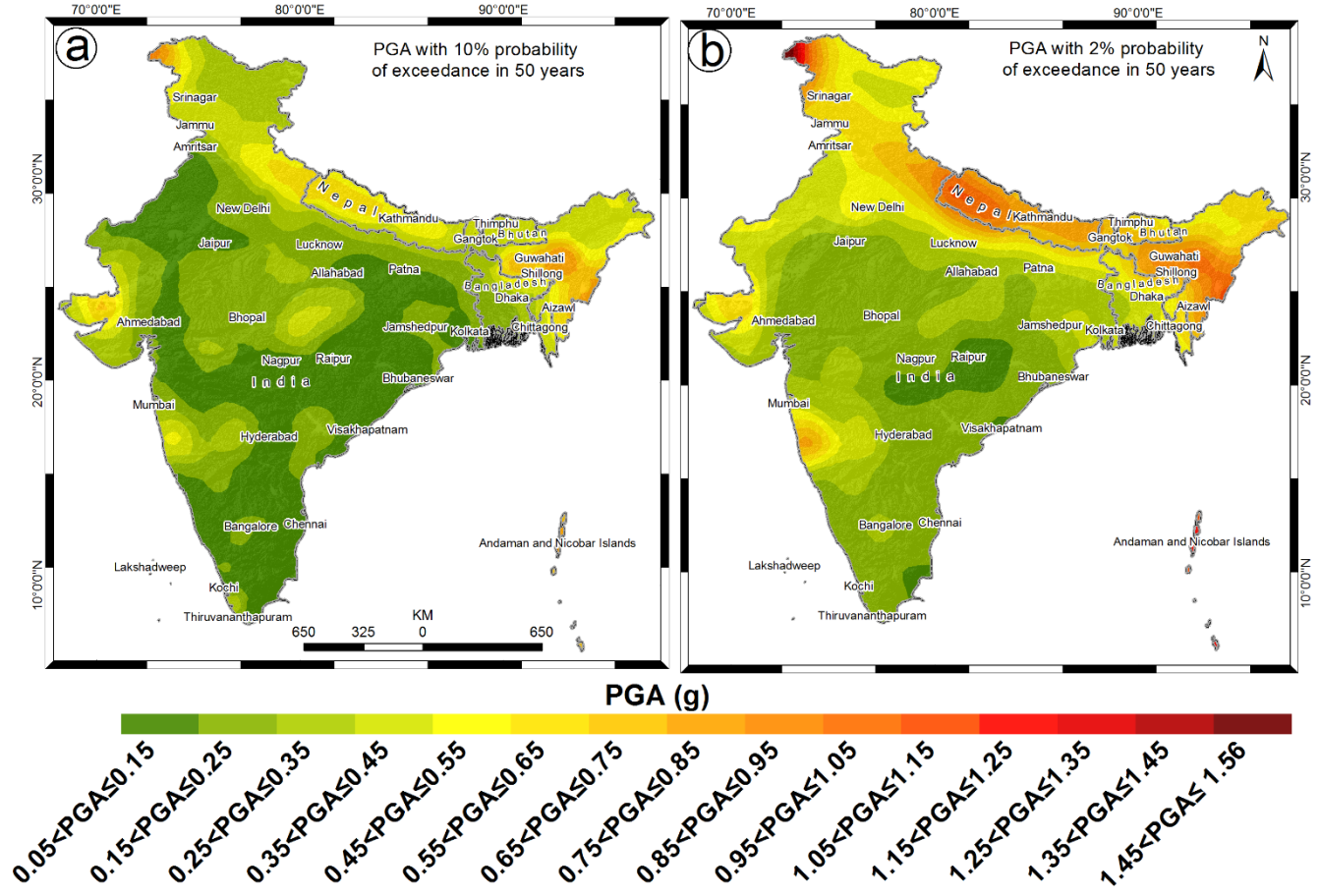

Figure 6 Probabilistic Seismic Hazard of India and its surrounding region in terms of Peak Ground Acceleration (PGA) at Bedrock level for (**a**) 10% Probability of exceedance in 50 years and (**b**) 2% Probability of exceedance in 50 years.

https://doi.org/10.5194/nhess-2022-66
Preprint. Discussion started: 22 March 2022

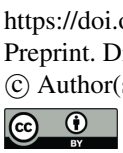

Natural Hazards and Earth System Sciences
Discussions
Open Access
EGU

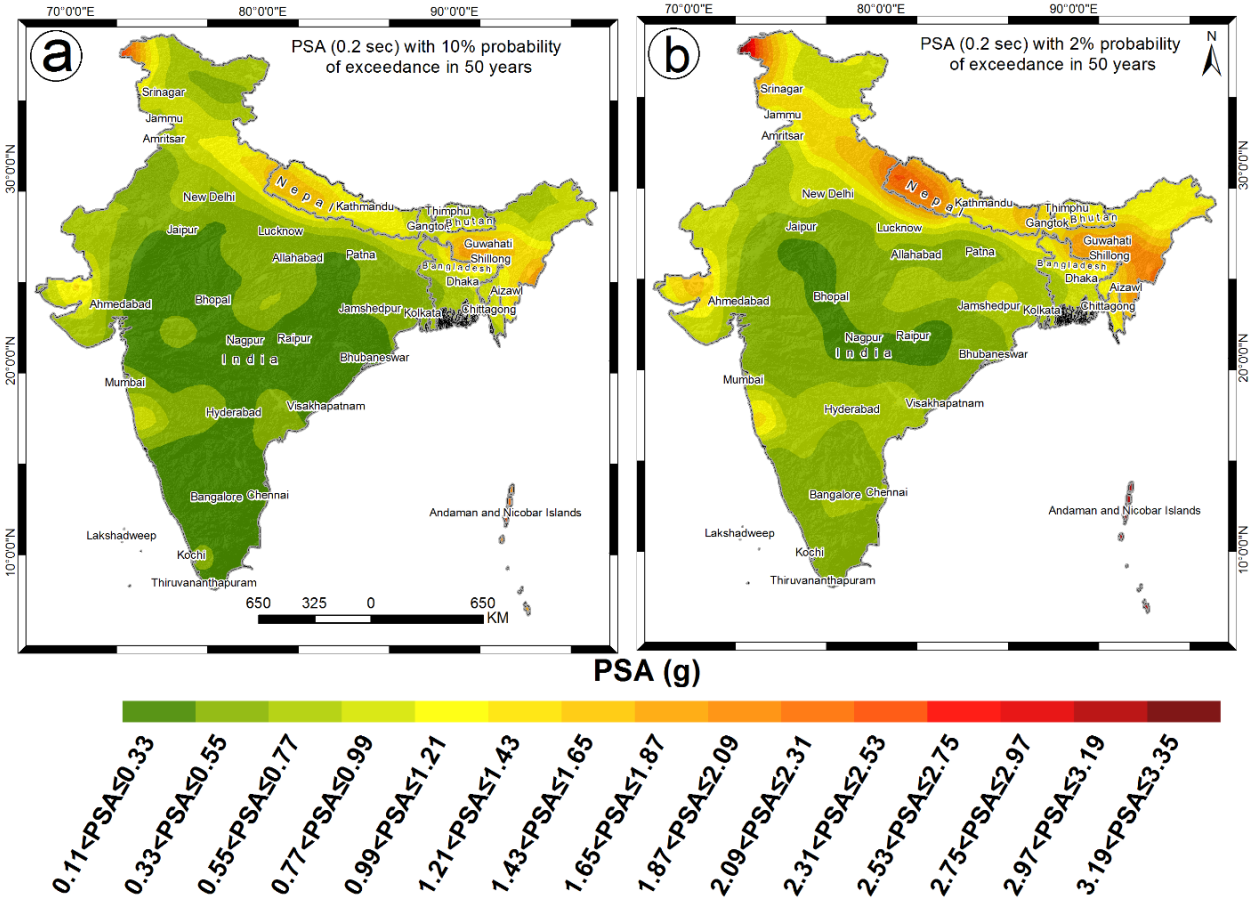

Figure 7 Probabilistic Seismic Hazard of India and its surrounding region in terms of Pseudo Spectral Acceleration (PSA) at Bedrock level for 0.2 sec period for (**a**) 10% Probability of exceedance in 50 years and (**b**) 2% Probability of exceedance in 50 years.

https://doi.org/10.5194/nhess-2022-66
Preprint. Discussion started: 22 March 2022

Natural Hazards and Earth System Sciences
Discussions

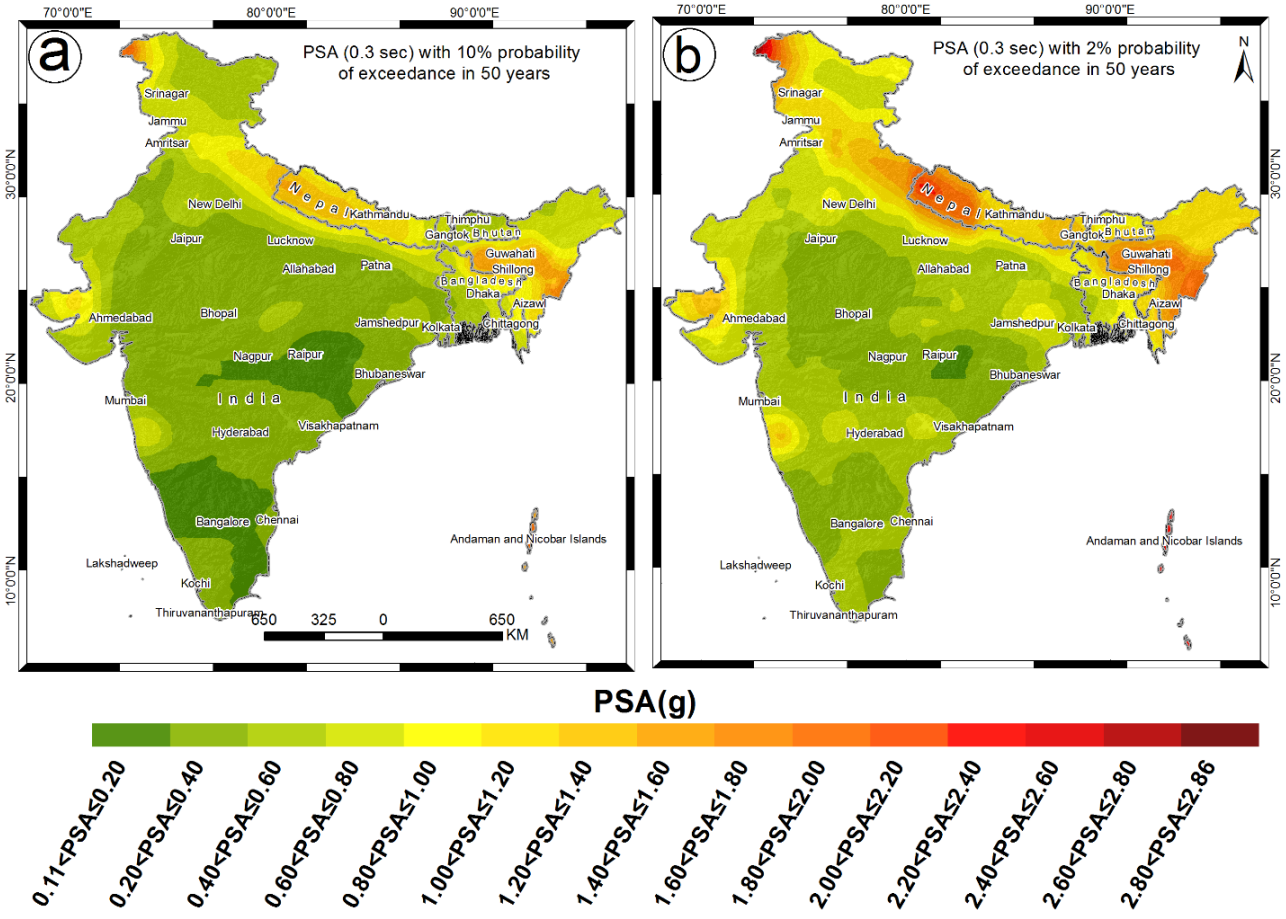

Figure 8 Probabilistic Seismic Hazard of India and its surrounding region in terms of Pseudo Spectral Acceleration (PSA) at Bedrock level for 0.3 sec period for (**a**) 10% Probability of exceedance in 50 years and (**b**) 2% Probability of exceedance in 50 years.

https://doi.org/10.5194/nhess-2022-66
Preprint. Discussion started: 22 March 2022

Natural Hazards and Earth System Sciences
Discussions

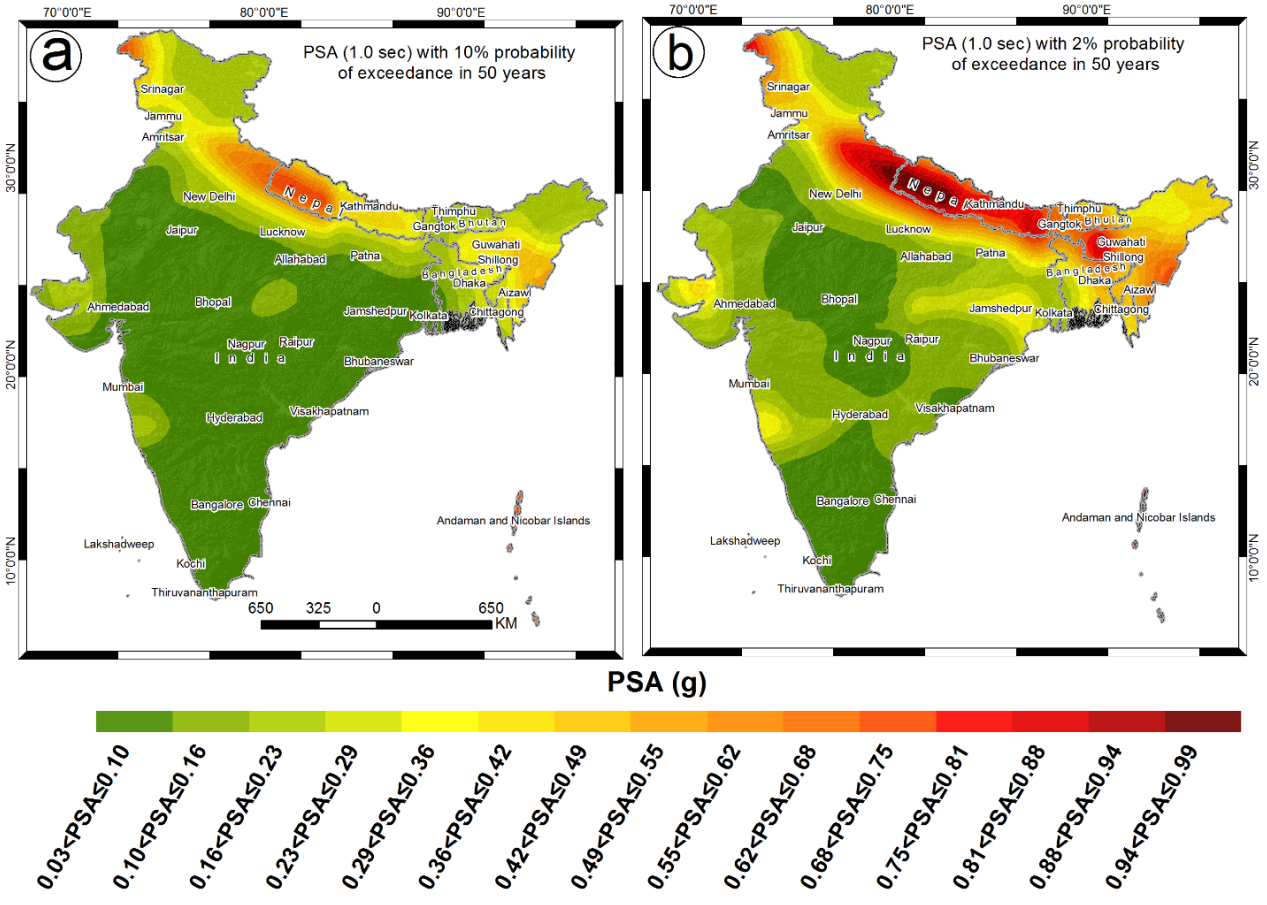

Figure 9 Probabilistic Seismic Hazard of India and its surrounding region in terms of Pseudo Spectral Acceleration (PSA) at Bedrock level for 1.0 sec period for (**a**) 10% Probability of exceedance in 50 years and (**b**) 2% Probability of exceedance in 50 years.

https://doi.org/10.5194/nhess-2022-66
Preprint. Discussion started: 22 March 2022

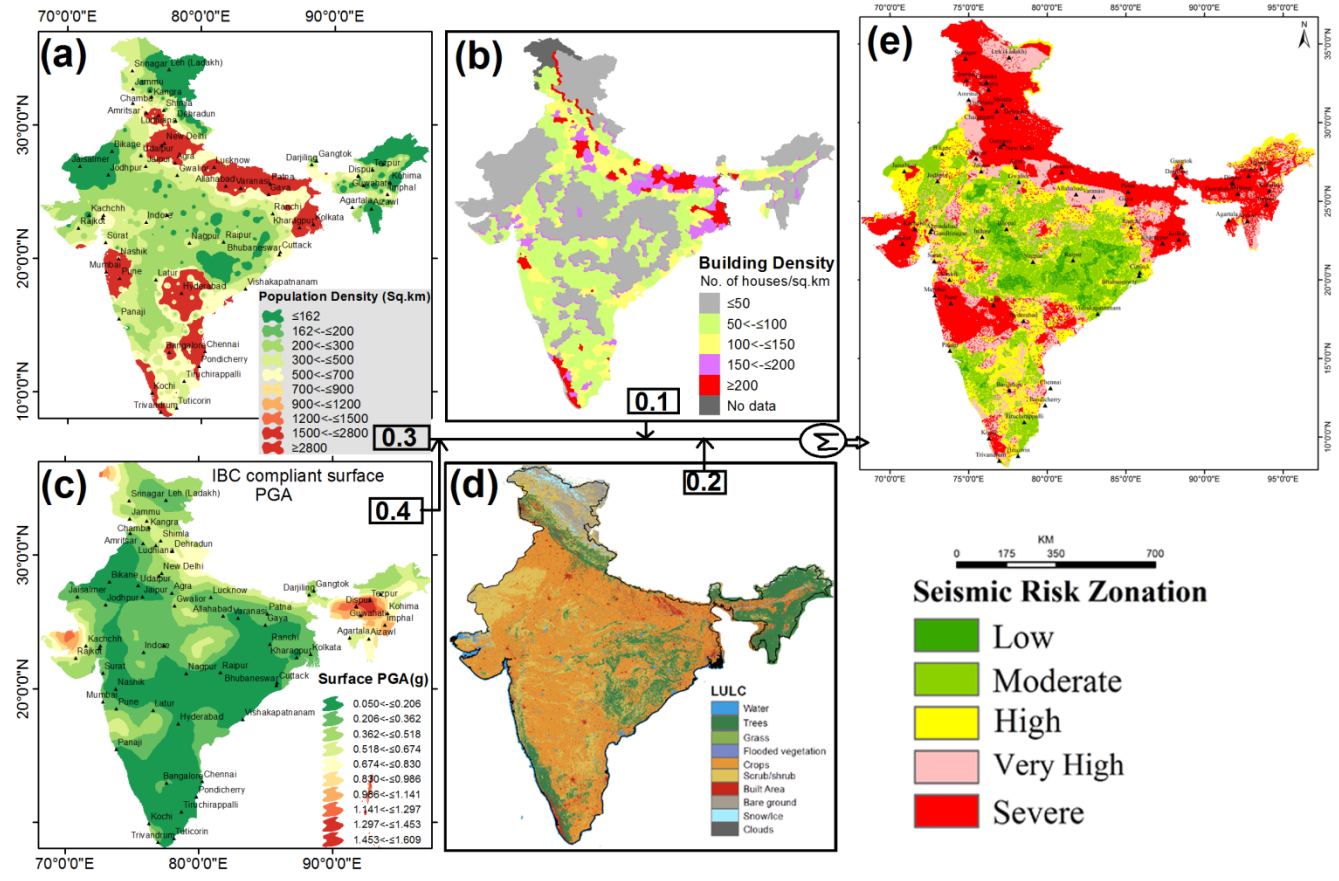

Figure 10 Seismic Risk Assessment of India on GIS platform through integration of (**a**) Population Density, (**b**) Building Density, (**c**) IBC compliant Surface PGA (in g) distribution with 10% probability of exceedance in 50 years and (**d**) Landuse/Landcover (LULC) thereby generating Socio-economic Seismic Risk Map of India as shown in (**e**). The weight assignment in the integration protocol is performed through pairwise comparison and expert judgement.

https://doi.org/10.5194/nhess-2022-66
Preprint. Discussion started: 22 March 2022

Natural Hazards and Earth System Sciences
Discussions

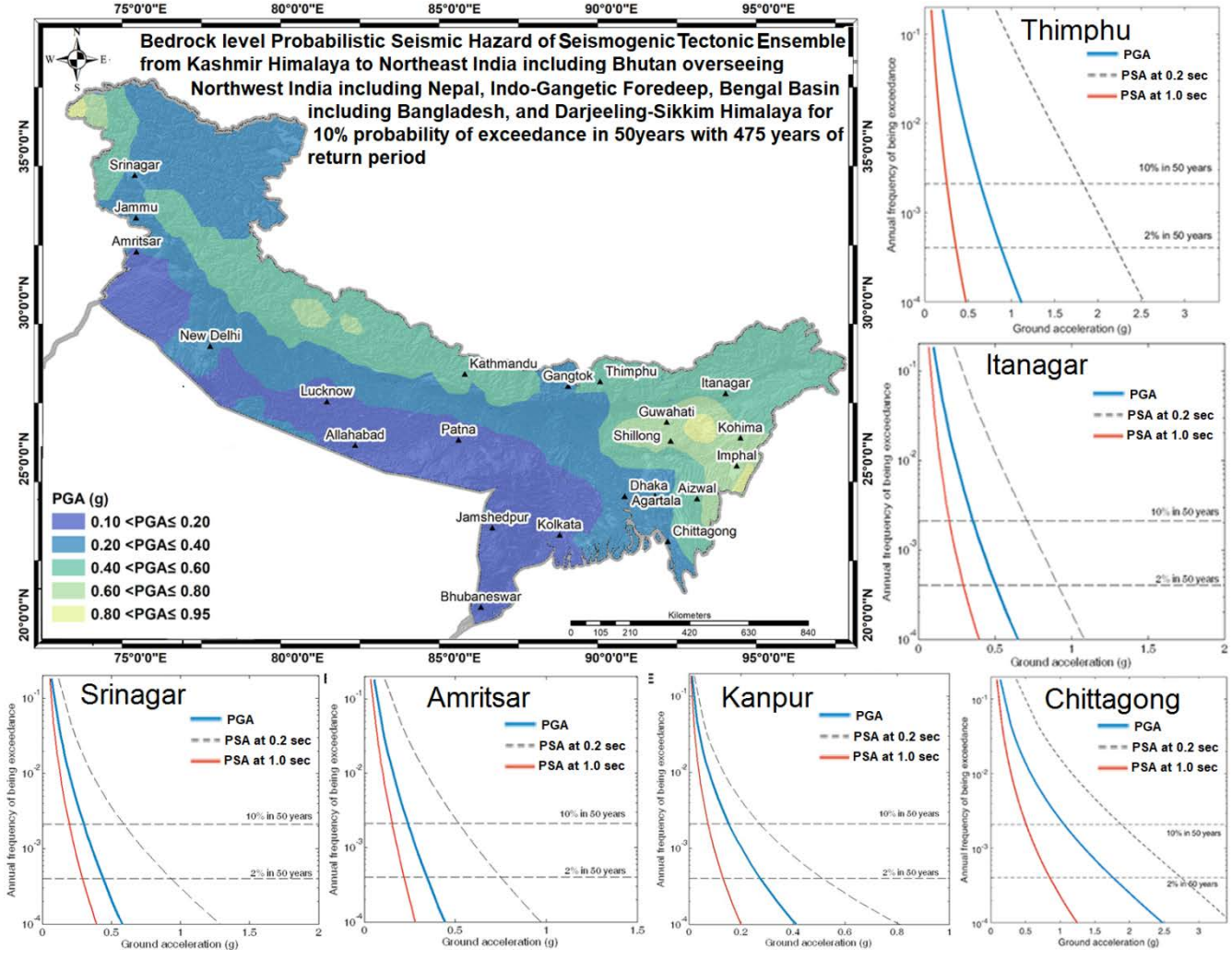

Figure 11 Bedrock level Probabilistic Seismic Hazard of the Seismogenic Tectonic Ensemble comprising of Kashmir Himalaya to Northeast India, which encompasses Northwest India, Nepal Himalaya, Indo-Gangetic Foredeep, Darjeeling-Sikkim Himalaya, Bengal Basin including Bangladesh and Bhutan Himalaya for 10% probability of exceedance in 50 years. Representative Hazard Curves generated for the Cities of Srinagar, Amritsar, Kanpur, Chittagong, Itanagar and Thimphu have also been depicted in the diagram.

https://doi.org/10.5194/nhess-2022-66
Preprint. Discussion started: 22 March 2022

Natural Hazards and Earth System Sciences
Discussions

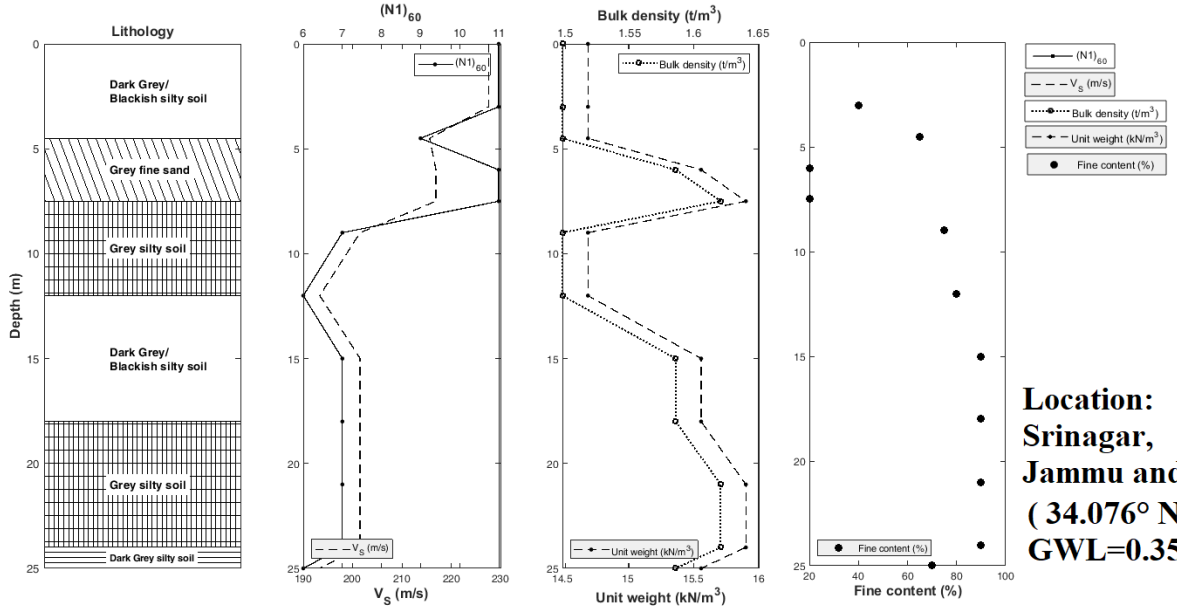

(a)

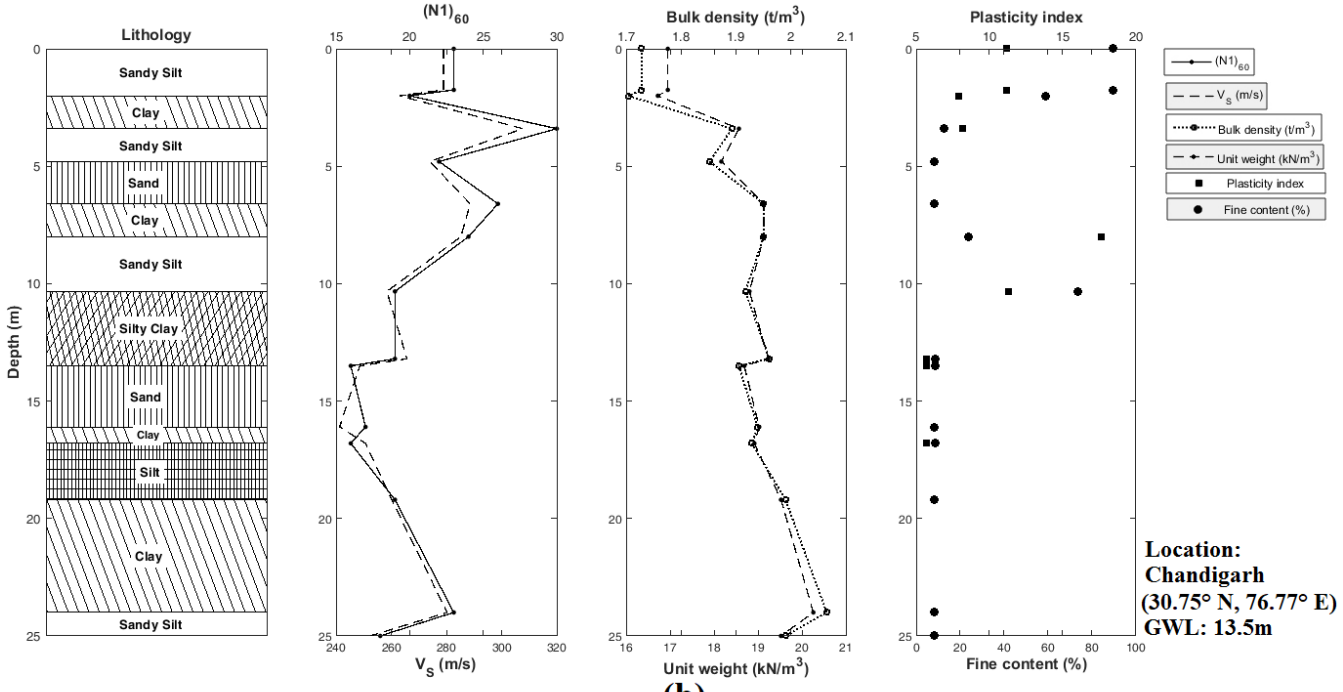

(b)

https://doi.org/10.5194/nhess-2022-66
Preprint. Discussion started: 22 March 2022

Natural Hazards and Earth System Sciences
Discussions

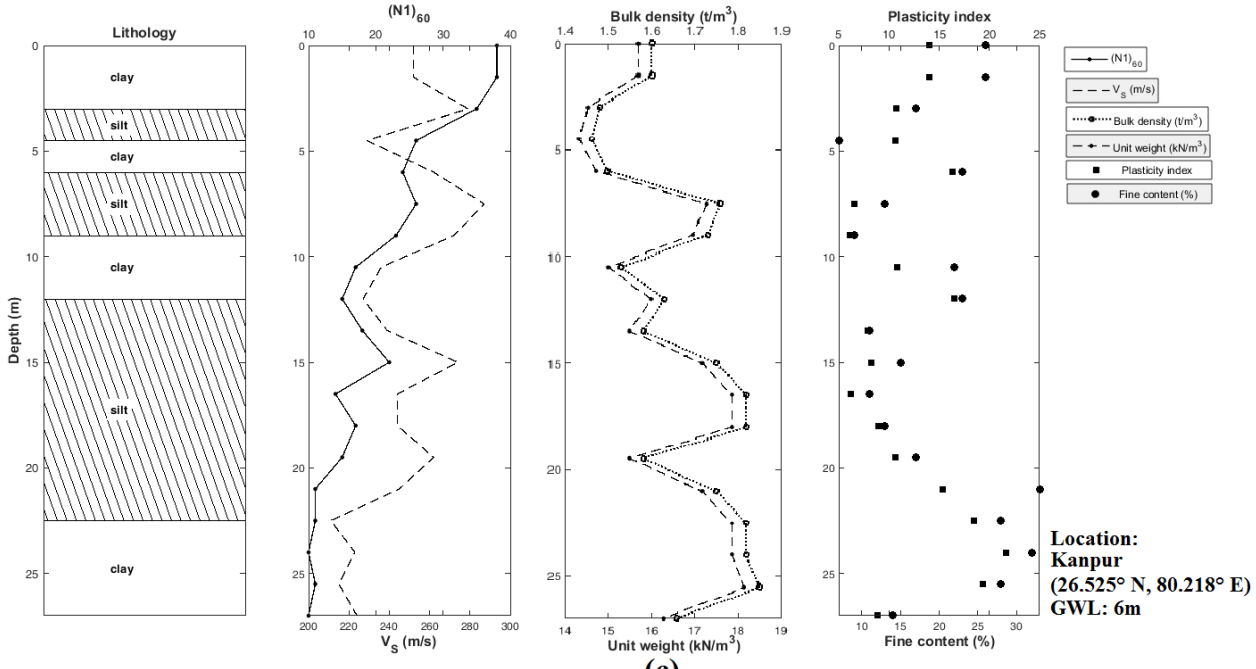

(c)

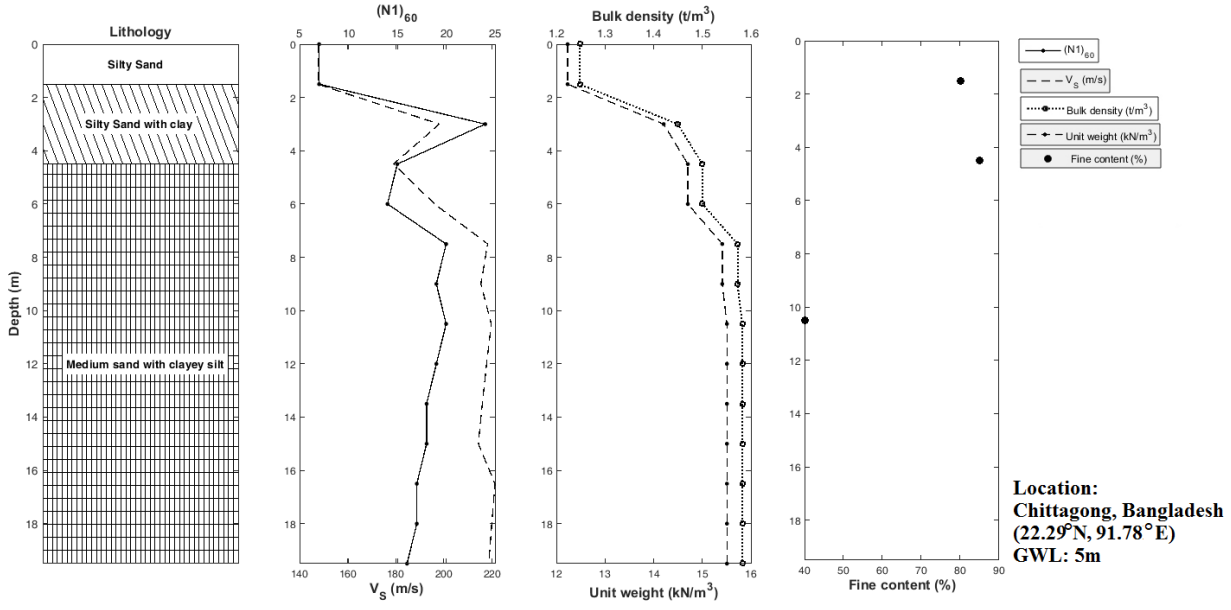

(d)

685

https://doi.org/10.5194/nhess-2022-66
Preprint. Discussion started: 22 March 2022

Natural Hazards and Earth System Sciences
Discussions

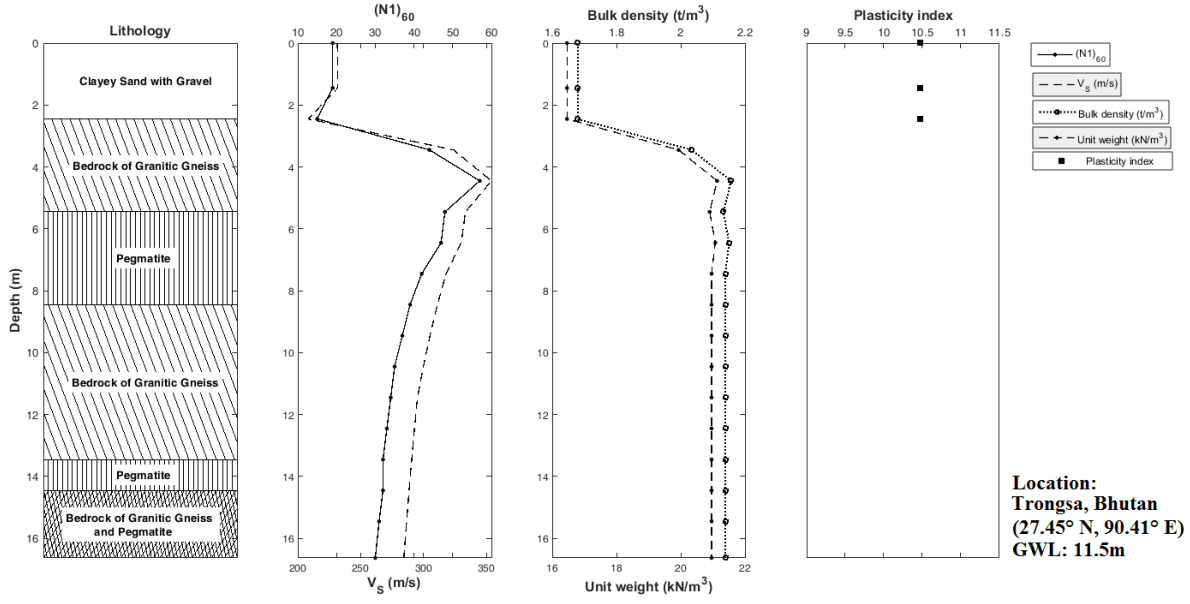

(e)

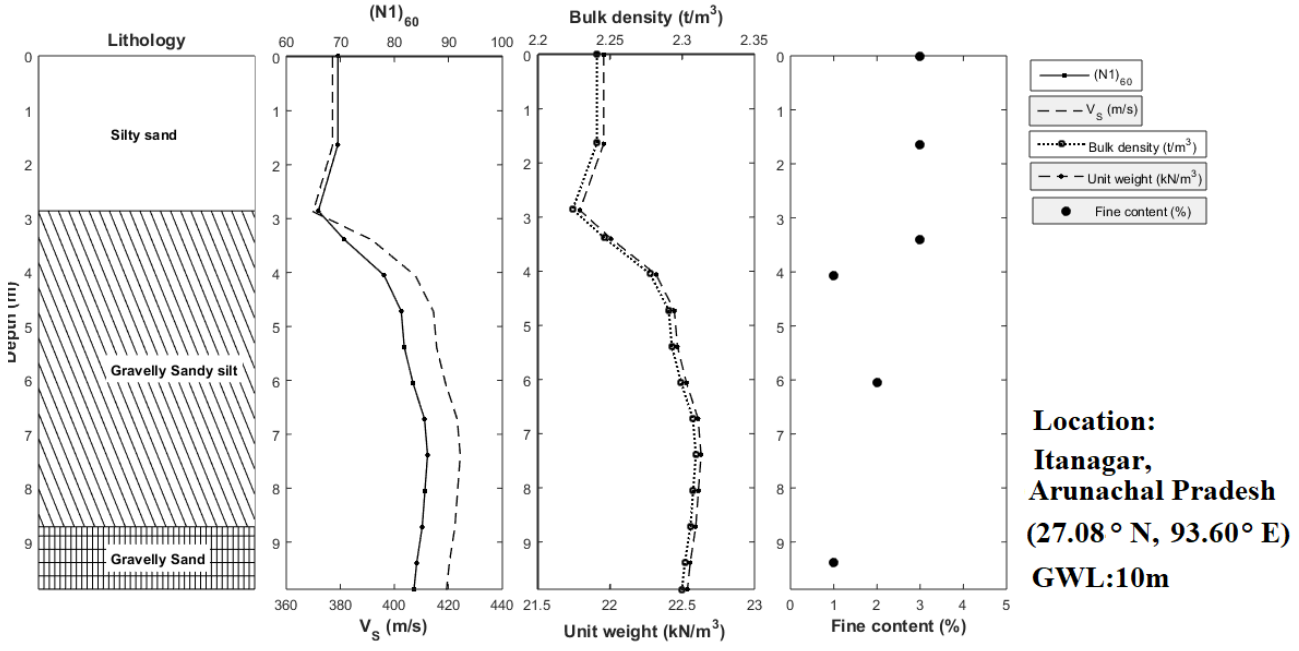

(f)

Figure 12 Sample Geotechnical data presenting depth-wise variation in lithology, corrected SPT-N, Shear wave velocity, Unit Weight, Bulk Density, Plasticity Index and Fine Content from representative drill holes at (**a**) Srinagar in Kashmir, (**b**) Chandigarh in Punjab, (**c**) Kanpur in Uttar Pradesh, (**d**) Chittagong in Bangladesh, (**e**) Gangtok in Sikkim and (**f**) Itanagar in Arunachal Pradesh.

https://doi.org/10.5194/nhess-2022-66
Preprint. Discussion started: 22 March 2022

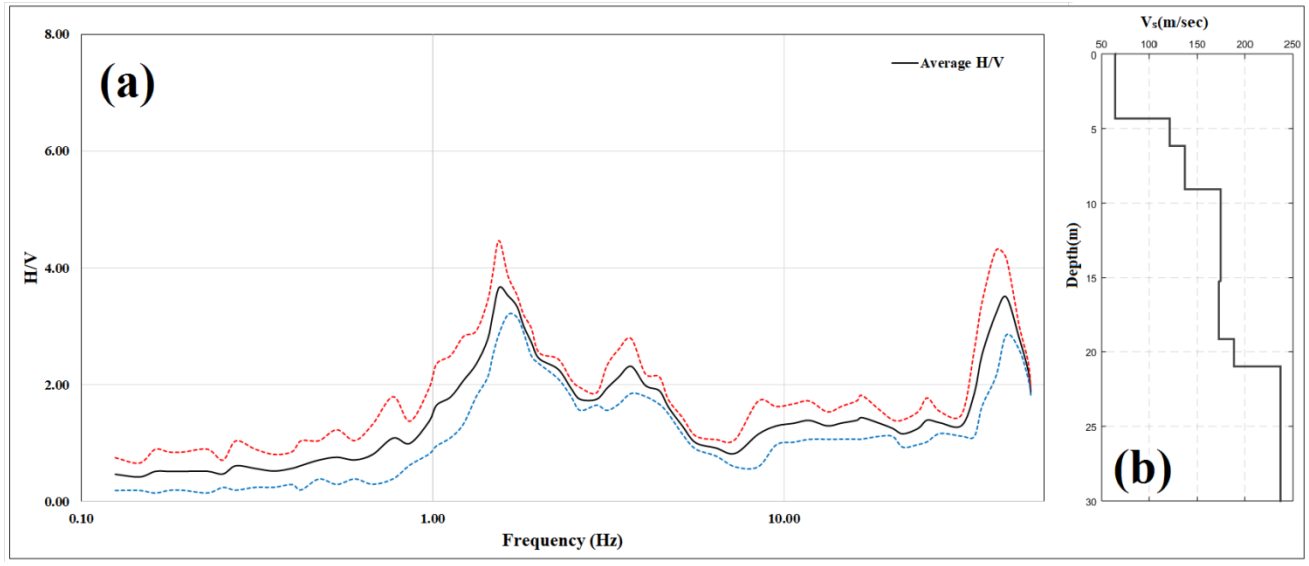

Figure 13 (**a**) Mean Nakamura Ratio computed from several Microtremor Survey conducted in the City of Agartala at various times of the day and (**b**) Inverted 1D Shear Wave velocity (in m/s) as obtained through inversion of the mean data-driven H/V curve.

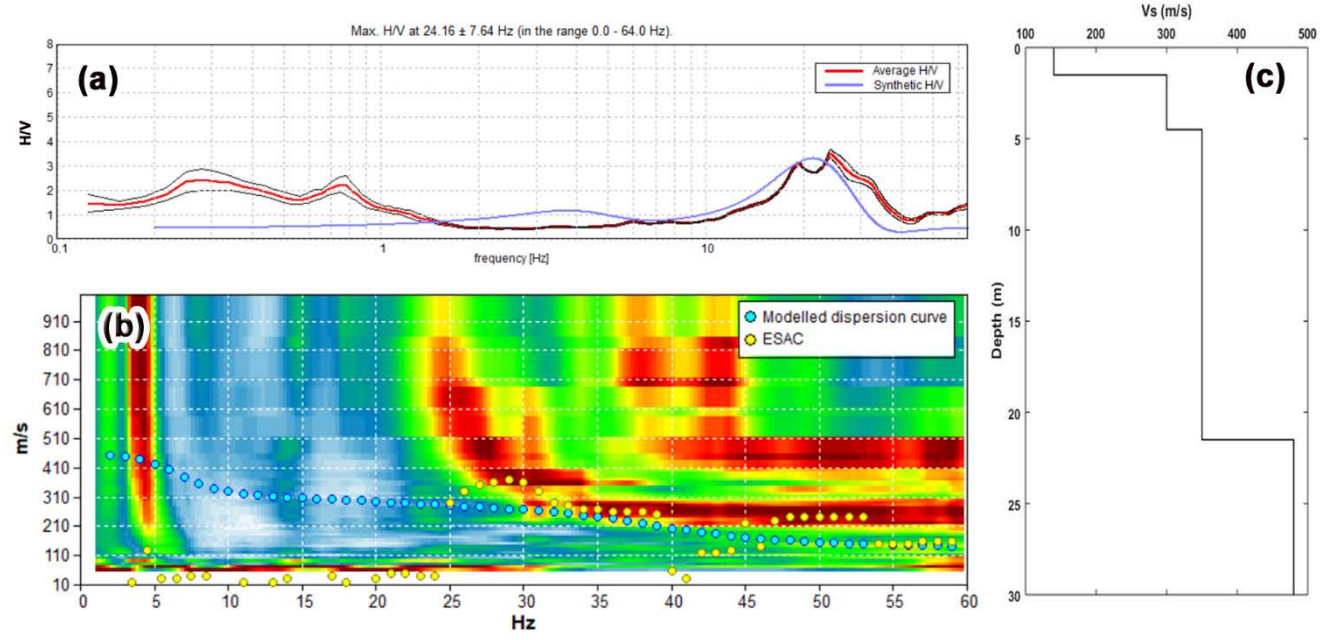

Figure 14 (**a**) Representative Ambient Noise driven H/V curve at Imphal in Manipur, (**b**) dispersion curves derived from SASW survey carried out in Imphal, Manipur and (**c**) 1D Shear wave velocity section of the subsurface for the City of Imphal in Manipur obtained from joint inversion of mean HVSR curve of diagram (**a**) and dispersion curve of diagram (**b**).

https://doi.org/10.5194/nhess-2022-66
Preprint. Discussion started: 22 March 2022

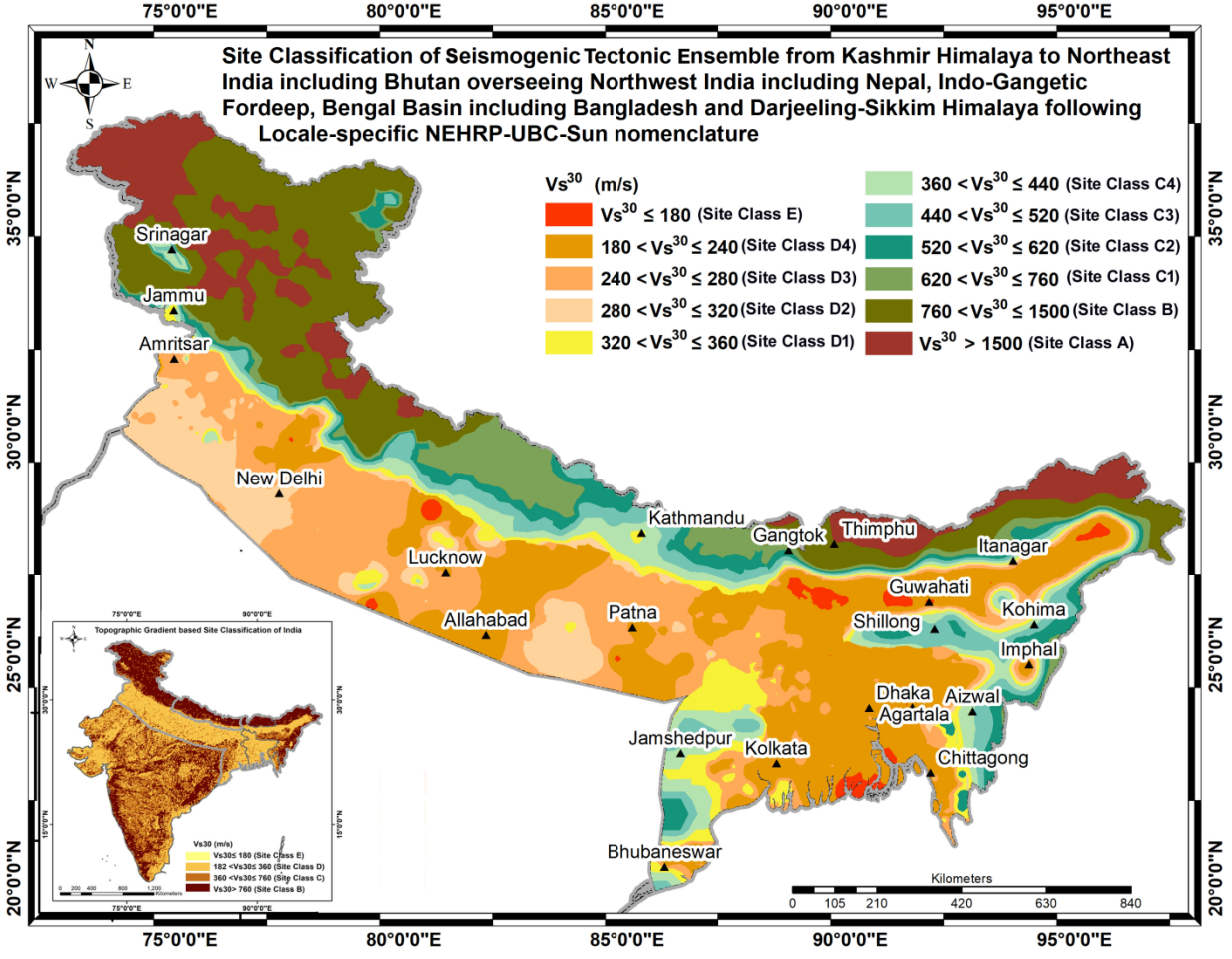

Figure 15 Site Classification map of the Seismogenic Tectonic Ensemble following the nomenclature of Sun et al. (2018) depicting the dominance of site class A, B, C1, C2, and C3 mostly in the hilly terrains of Kashmir Himalaya, Northwest India, Nepal Himalaya, Darjeeling-Sikkim Himalaya, Northeast India and Bhutan Himalaya, while site class C4 and D1 are predominantly seen in the plateau region of western part of Bengal Basin and Shillong Plateau of Northeast India, whereas, D2, D3, D4 and E/F are seen in the alluvial plains of Northwest India, Indo-Gangetic Foredeep, Bengal Basin and Brahmaputra Valley of Northeast India. The topographic gradient based site classification map of India and its surrounding region following Nath et al. (2013) is given in the inset of this diagram.

https://doi.org/10.5194/nhess-2022-66
Preprint. Discussion started: 22 March 2022

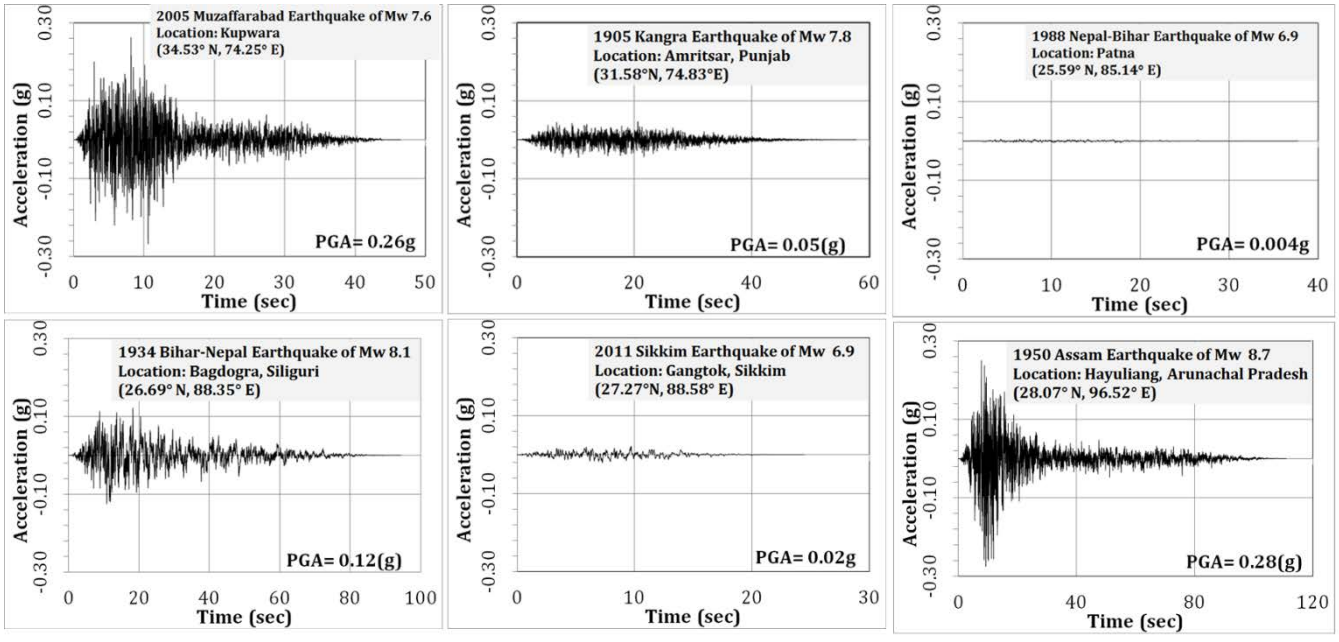

Figure 16 Synthesized strong ground motion at engineering bedrock level using EXSIM software of Boore (2009) at (**a**) Kupwara in Jammu and Kashmir for 2005 Kashmir earthquake of M_w 7.6, (**b**) Amritsar in Punjab for 1905 Kangra earthquake of M_w 7.8, (**c**) Patna in Bihar for 1988 Nepal-Bihar earthquake of M_w 6.9, (**d**) Siliguri in West Bengal for 1934 Bihar-Nepal earthquake of M_w 8.1, (**e**) Gangtok in Sikkim for 2011 Sikkim earthquake of M_w 6.9 and (**f**) Hayuliang in Arunachal Pradesh for 1950 Assam earthquake of M_w 8.7.

https://doi.org/10.5194/nhess-2022-66
Preprint. Discussion started: 22 March 2022

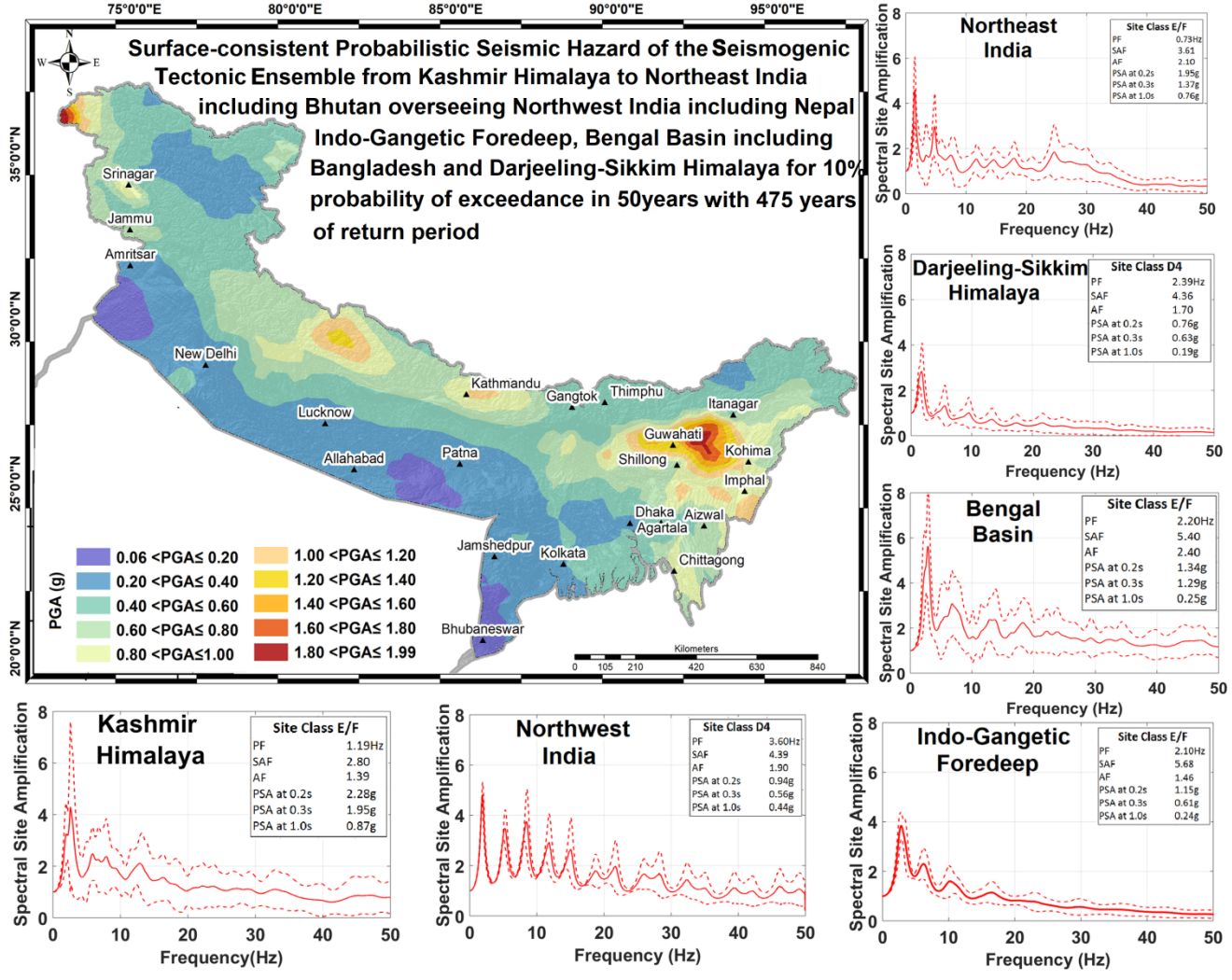

715 **Figure 17** Surface-consistent Probabilistic Seismic Hazard of the Seismogenic Tectonic Ensemble comprising of Kashmir Himalaya to Northeast India covering the entire stretch of Northwest India, Nepal Himalaya, Indo-Gangetic Foredeep, Bengal Basin containing both West Bengal and Bangladesh, Darjeeling-Sikkim Himalaya and Bhutan Himalaya for 10% probability of exceedance in 50 years. Generic site response curves (red bold line) ±1 Standard Deviation (red dotted lines) and associated site parameters mostly in the site class E/F/D4 in each Seismogenic Tectonic Province are also presented in 720 the diagram.

https://doi.org/10.5194/nhess-2022-66
Preprint. Discussion started: 22 March 2022

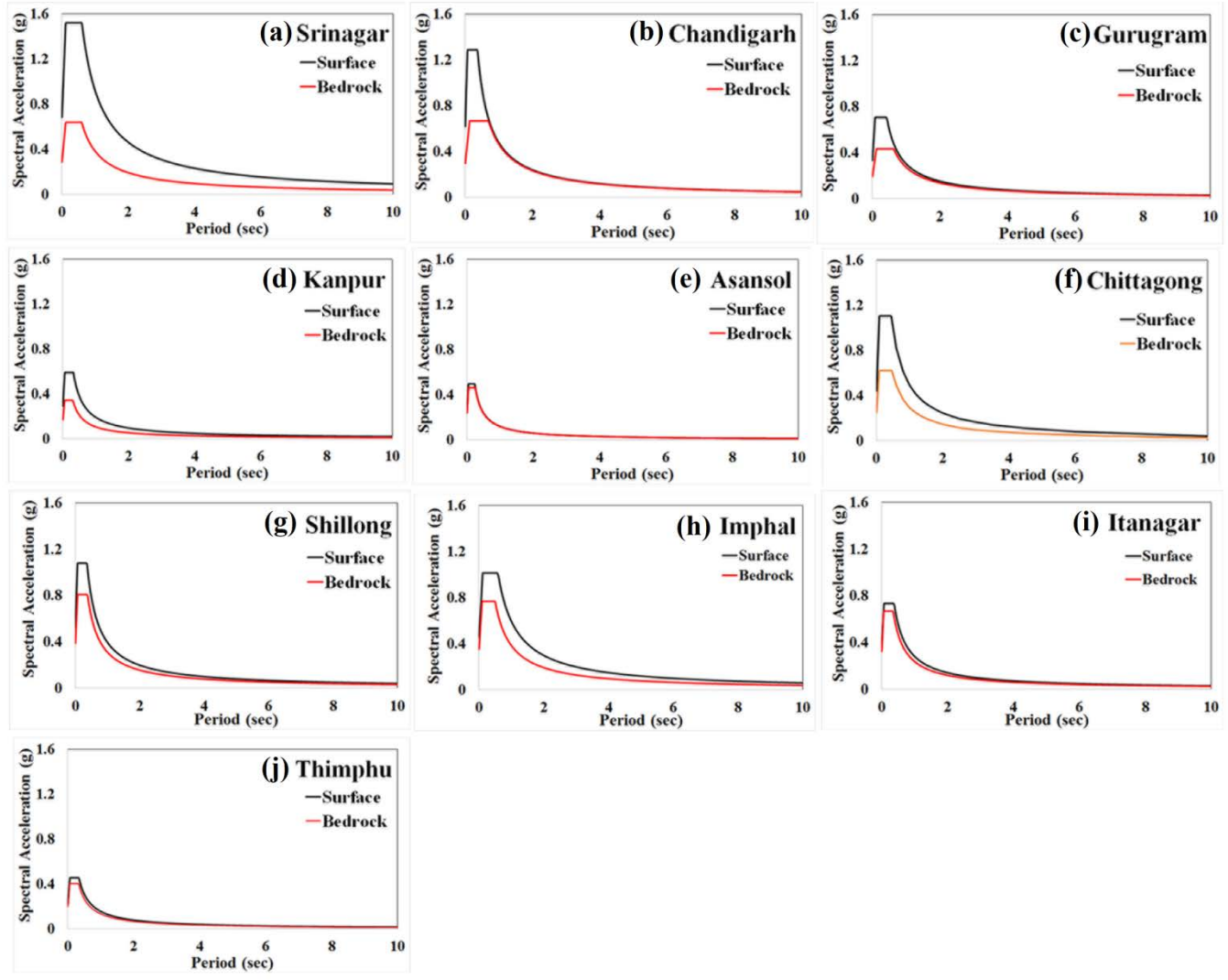

Figure 18 Representative Design response spectra (5% damped) worked out at both engineering bedrock and surface-consistent level using PSA at 1.0sec and 0.2sec with 10% probability of exceedance in 50 years are shown for the city of (**a**) Srinagar in Jammu and Kashmir, (**b**) Chandigarh in Punjab, (c) Gurugram in Haryana, (**d**) Kanpur in Uttar Pradesh, (**e**) Asansol in West Bengal, (**f**) Chittagong in Bangladesh, (**g**) Shillong in Meghalaya, (**h**) Imphal in Manipur, (**i**) Itanagar in Arunachal Pradesh and (**j**) Thimphu in Bhutan.

https://doi.org/10.5194/nhess-2022-66
Preprint. Discussion started: 22 March 2022

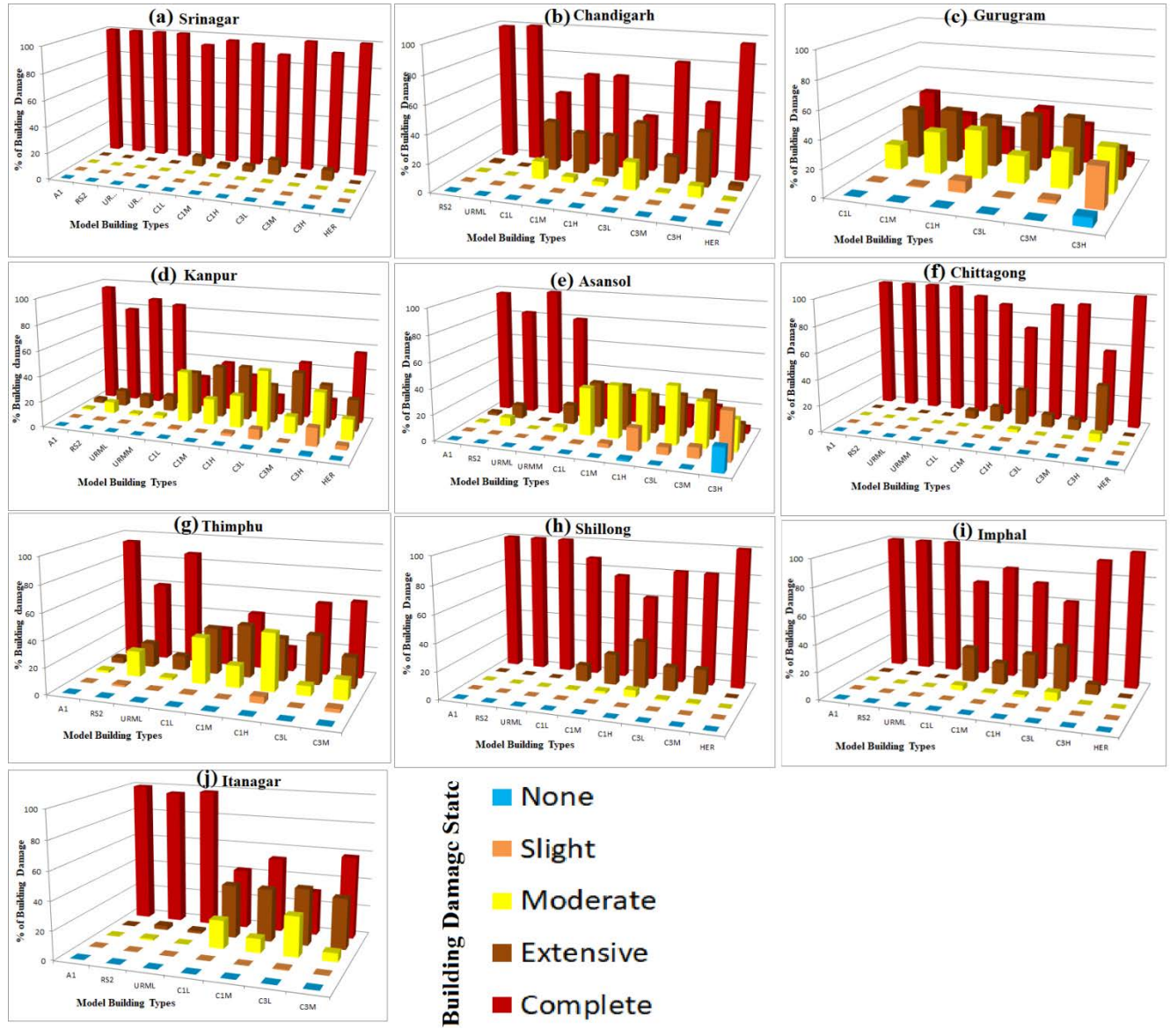

Figure 19 Representative Discrete damage probability estimated using SELENA–based Capacity Spectrum Method (Molina and Lindholm, 2005; Molina et al., 2010) in terms of "None", "Slight", "Moderate", "Extensive", and "Complete" for the model building types viz. A1, RS2, URML, URMM, C1L, C1M, C1H, C3L, C3M, C3H and HER (FEMA, 2000; WHE-PAGER, 2008) are shown for (**a**) Srinagar in Jammu and Kashmir, (**b**) Chandigarh in Punjab, (**c**) Gurugram in Haryana, (**d**) Kanpur in Uttar Pradesh, (**e**) Asansol in West Bengal, (**f**) Chittagong in Bangladesh, (**g**) Thimphu in Bhutan, (**h**) Shillong in Meghalaya, (**i**) Imphal in Manipur and (**j**) Itanagar in Arunachal Pradesh for the surface-consistent probabilistic seismic hazard for 10% probability of exceedance in 50years.

https://doi.org/10.5194/nhess-2022-66
Preprint. Discussion started: 22 March 2022

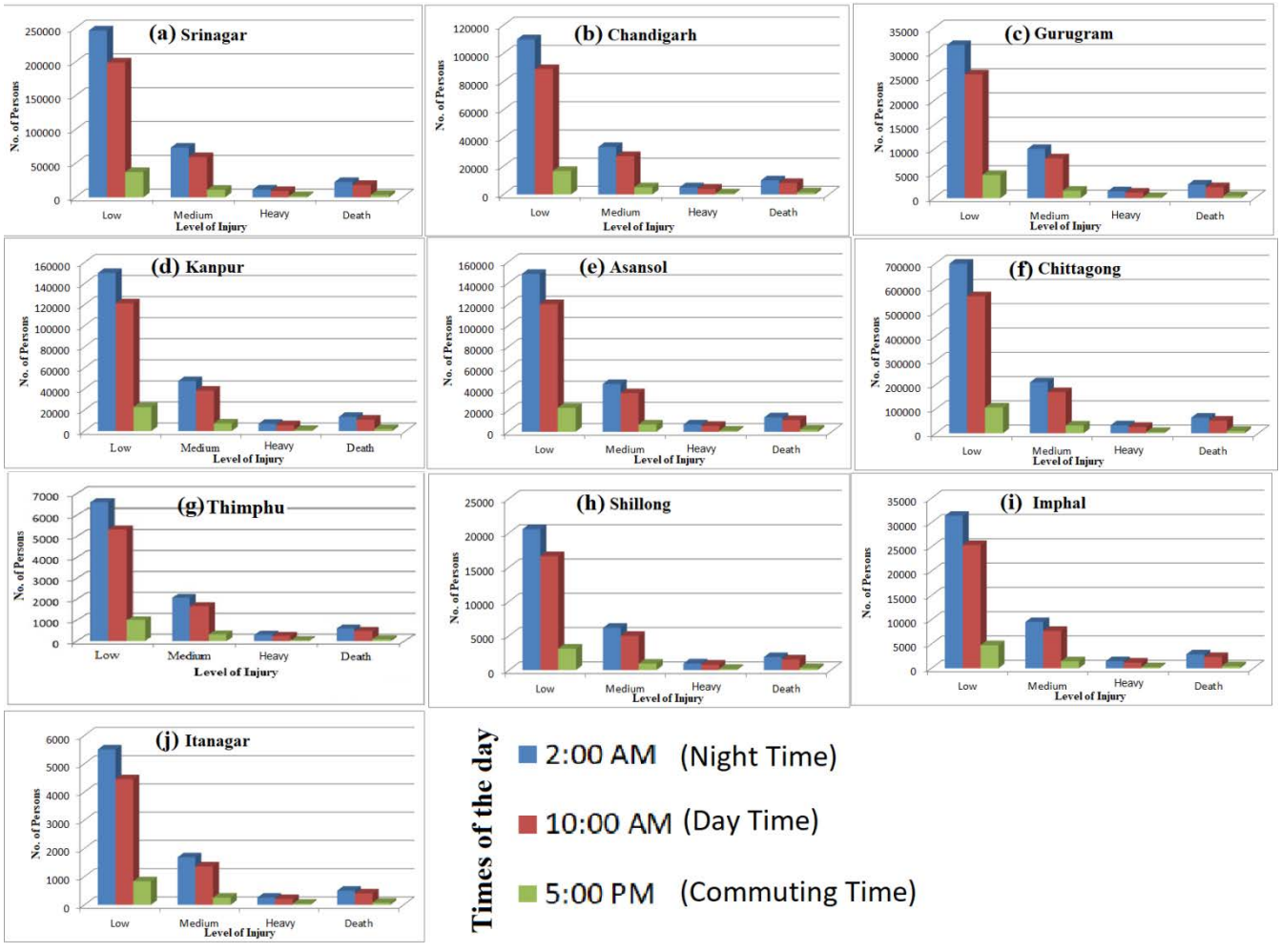

Figure 20 Number of Human Casualties at different levels of injury in three different times of the day for (**a**) Srinagar in Jammu and Kashmir, (**b**) Chandigarh in Punjab, (**c**) Gurugram in Haryana, (**d**) Kanpur in Uttar Pradesh, (**e**) Asansol in West Bengal, (**f**) Chittagong in Bangladesh, (**g**) Thimphu in Bhutan, (**h**) Shillong in Meghalaya, (**j**) Imphal in Manipur and (**h**) Itanagar in Arunachal Pradesh for the surface-consistent probabilistic seismic hazard for 10% probability of exceedance in 50years.

https://doi.org/10.5194/nhess-2022-66
Preprint. Discussion started: 22 March 2022

Natural Hazards and Earth System Sciences Discussions

Table 1: Percentage of indoor and outdoor population dependent on the time of the day (Molina et al., 2010; Nath et al., 2015; Ghatak et al., 2017)

Occupancy Class	**Day (%) (at 10:00 AM)**	**Commuting (%) (at 5:00 PM)**	**Night (%) (at 2:00 AM)**
Indoor	90	36	98
Outdoor	10	64	2
Total	100	100	100

Table 2. Representation of Fatality index in Srinagar, Chandigarh, Gurugram, Kanpur, Asansol, Chittagong, Thimphu, Shillong, Imphal and Itanagar.

Serial No.	**Cities**	**Human Casualty (in number of injured persons)**		
		2AM	**10AM**	**5PM**
1.	Srinagar	354390	286376	53695
2.	Chandigarh	158822	128341	24064
3.	Gurugarm	45890	37083	6953
4.	Kanpur	217713	175930	32987
5.	Asansol	213984	172916	32422
6.	Chittagong	1003845	811187	152098
7.	Thimphu	9552	7719	1447
8.	Shillong	29527	23860	4473
9.	Imphal	45229	36548	6852
10.	Itanagar	7942	6418	1203